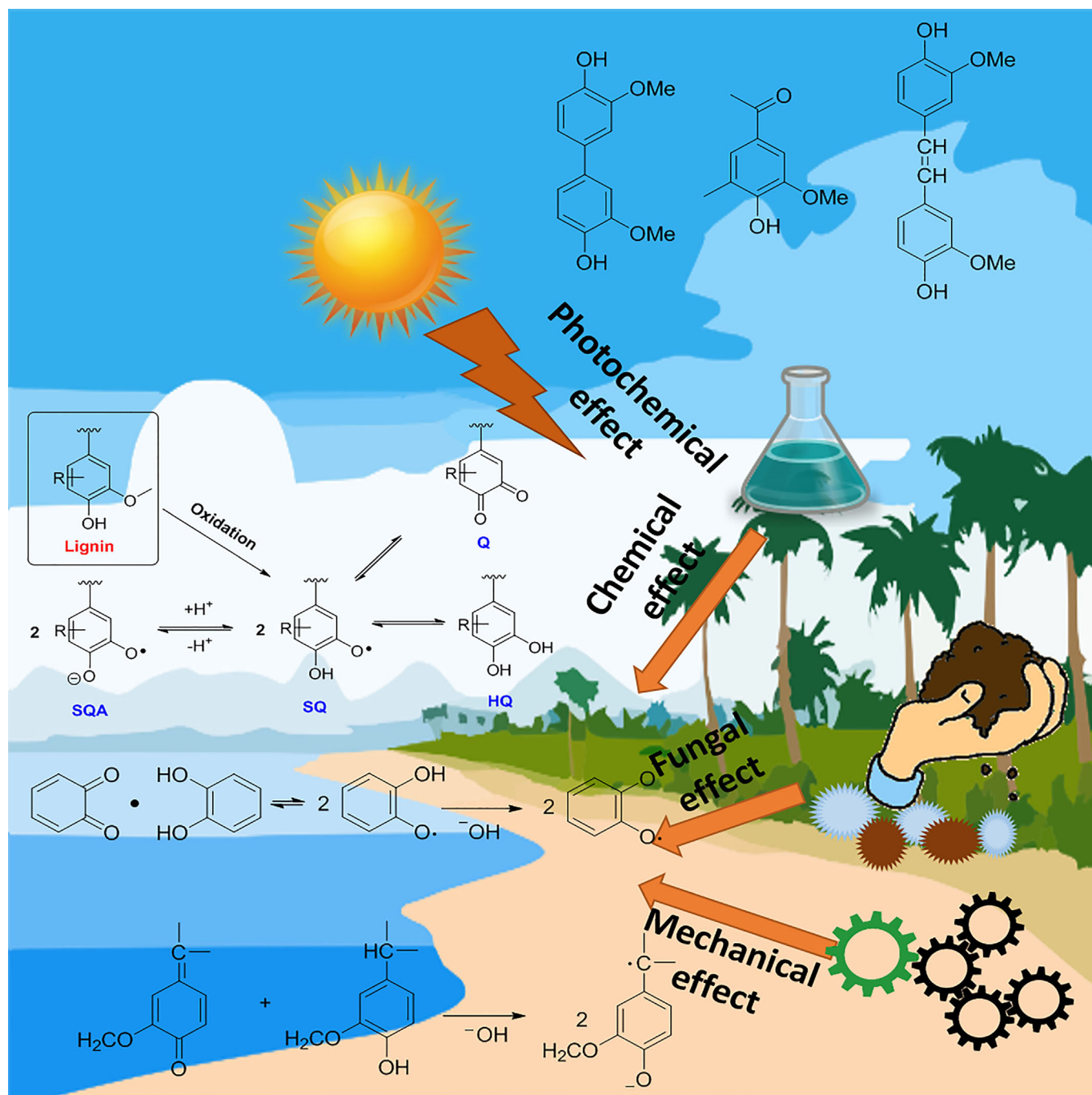


Stable Organic Radicals in Lignin: A Review

Shradha V. Patil and Dimitris S. Argyropoulos^{*[a]}



Lignin and the quest for the origin of stable organic radicals in it have seen numerous developments. Although there have been various speculations over the years on the formation of these stable radicals, researchers have not been able to arrive at a solid, unequivocal hypothesis that applies to all treatments and types of lignin. The extreme complexity of lignin and its highly aromatic, cross-linked, branched, and rigid structure has made such efforts rather cumbersome. Since the early 1950s, researchers in this field have dedicated their efforts to the establishment of methods for the detection and determination of spin content, theoretical simulations, and reactions on

model compounds and spin-trapping studies. Although a significant amount of published research is available on lignin or its model compounds and the reactive intermediates involved during various chemical treatments (pulping, bleaching, extractions, chemical modifications, etc.), the literature provides a limited view on the origin, nature, and stability of such radicals. Consequently, this review is focused on examining the origin of such species in lignin, factors affecting their presence, reactions involved in their formation, and methods for their detection.

1. Introduction

1.1. Structural aspects of lignin and associated stable radicals

Prior to examining details pertaining to the subject matter of this review, it is important to briefly summarize the key structural features of lignin to create the foundations for further discussion. Chemically, native lignin is an intricate aromatic polymer with some phenolic character and plant-specific composition and linkage motifs.^[1,2] Literature precedence highlights that lignin lacks an organized primary structure, but it is better represented by chains of phenylpropanoid polyphenols. These chains are primarily connected by arylglycerol ether bonds between sinapyl alcohol (S type), coniferyl alcohol (G type), and *para*-coumaryl alcohol (H type) units (Figure 1).^[3,4] A recent

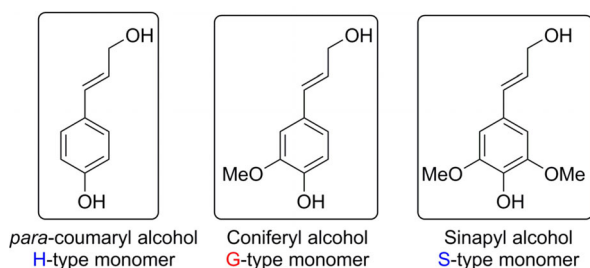


Figure 1. Structures for types of monomers present in lignin (*para*-coumaryl (H), coniferyl (G), and sinapyl (S) alcohol).^[10,11]

report also discussed the oligomeric structure of these biopolymeric chains.^[5] Each of these types could dominate in lignin, depending on the type of plant or wood species. As such, the lignin of gymnosperms is believed to contain almost exclusively G-type precursors (G-lignin); dicotyledonous (angiosperms) a mixture of G and S (GS-lignin); and that of monocotyledonous species consists of G, S, and H precursors.^[6]

Monolignol radicals are thought to be initially generated, which lead to the formation of various binding types, and thus, the undisputedly rich complexity of lignin.^[7,8] The β -O-4 coupling of monolignols with other radicals offer quinone methide intermediates that function as new monomers.^[9] The quinone methide intermediates are stabilized by nucleophiles (water, neutral sugars, uronic acids, etc.) to create oligomers. Therefore, the formation of lignin is rather seen as a random series of polymerization–termination reactions instead of a systematic living radical polymerization process. These random series of polymerization–termination reactions involve continuously growing oligomers, which produce a highly polydisperse biomaterial in the absence of a series of conventional repeating units. The relative abundance of H/G/S types of units and distribution of interunit linkages resulting from coupling reactions defines the composition of the final biopolymer.

Traditionally, the constitutional scheme for lignin was based on information collected from different sources, for instance, analytical studies on milled spruce wood lignin,^[12] biochemical experiments related to H-/G-/S-type moieties and their phenolic glucosides, and lignin degradation studies. These studies provided a comprehensive understanding of the structural features and reactivity of lignin macromolecule. Analytical data revealed valuable facts about the elemental composition of lignin; its methoxy group content; other ether linkages; the types and amounts of various hydroxyl, carbonyl, and lactone groups; and the types of biphenyl or other linkages.^[13,14] Biochemical experiments involved three cinnamyl alcohols (H, G, S) and their phenolic glucosides: *p*-glucocoumaryl alcohol, coniferin, and syringin (a mixture of geometric isomers with no *cis*–*trans* isolation,^[15] Figure 2). These glucosides are believed to be present in the cambial sap and in spruce wood; coniferin is the most abundant of all. Small amounts of coniferaldehyde, dilignols, and trilignols were also detected in spruce wood cambial sap. The degradation of lignin under strong alkali conditions, followed by methylation and/or oxidation, has offered information on the various bonding patterns.^[16–18] In addition, acidolysis–fractionation has also been used to elucidate fundamental structural features, such as phenylcoumaran and arylglycerol β -aryl ether.^[17,19]

This groundwork and the new NMR-based understanding of each of these structures and their related abundancy deductions made it possible to construct a recent spruce

[a] S. V. Patil, Prof. D. S. Argyropoulos
Departments of Forest Biomaterials and Chemistry
North Carolina State University, 2820 Faucette Drive
Raleigh, NC 27695-8005 (USA)
Fax: (919)-515-6302
E-mail: dsargyro@ncsu.edu

constitutional scheme (Figure 3). This scheme satisfactorily accommodated many other facts of lignin chemistry.

As mentioned earlier, for decades, the prevailing opinion about lignin was that it was a statistical biopolymer (or random polymer with distribution of chains of various lengths) with no specific structural formula, but could only be represented by structural schemes of repeating units detected by various studies.^[20] Various methods and chemical treatments

Dimitris S. Argyropoulos is Professor of Chemistry with the Departments of Chemistry and Forest Biomaterials at North Carolina State University. Recent cross-appointments of his include his affiliations as a Finland Distinguished Professor of Chemistry with the Department of Chemistry at the University of Helsinki in Finland and his visiting Distinguished Professorship with the Centre of Excellence for Advanced Materials Research, Jeddah, Saudi Arabia.



He received his Ph.D. in organic chemistry from McGill University in Montreal, Canada, where he also served as a PAPRICAN (Pulp & Paper Research Institute of Canada) professor with the Chemistry Department. He is a Fellow of the International Academy of Wood Science and a Fellow of the Canadian Institute of Chemistry, and he serves as an editor and on the editorial boards of five scientific journals. He has served as the Division Chair and Secretary of the Cellulose and Renewable Materials of the American Chemical Society. The work of his group focuses on the organic chemistry of wood components and the development of novel analytical methods and new chemistries for transforming carbon present in our trees toward producing valuable chemicals, materials, and energy.

Shradha V. Patil graduated with a Master of Science (M.Sc.) degree from the University of Pune in 2006 with a major in organic chemistry. She joined the Department of Chemistry for a Ph.D. program in August 2008 at Virginia Polytechnic Institute and State University under the supervision of Prof. James M. Tanko, with a focus on living free radical polymerization methods for C–H bond functionalization reactions of hydrocarbons and ethers



under metal-free conditions. After completing her Ph.D. in April 2013, she worked as a Postdoctoral Researcher at Virginia Polytechnic Institute and State University with Prof. Harry W. Gibson, where she worked on the synthesis of conjugated-conducting macromolecules for applications in organic solar cells, and later at North Carolina State University with Prof. Argyropoulos, where she worked on chemical modifications on lignocellulosic biomaterials for better thermoplastic properties and carbon fibers. Her future research interests include lignocellulosic biopolymer modifications for applications in advanced materials and sustainable solutions.

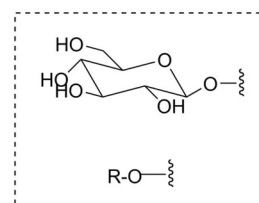
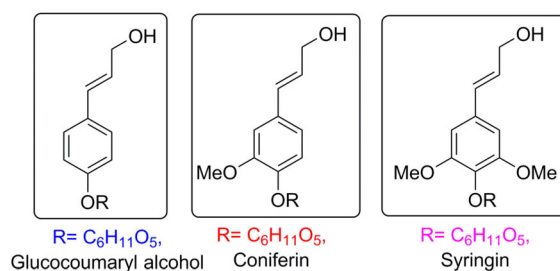


Figure 2. Phenolic glucoside precursors (adapted with permission from Elsevier, Copyright 1963).^[15]

were utilized to comprehend the structural and reactivity details of lignin. Herein, we provide a concise overview of the processes that play a crucial role in defining the radical content of lignin, including biological origin, natural degradation, chemical treatments, and mechanical treatments.

2. Origin of Stable Radicals in Lignin

2.1. Effect of botanical origin and natural processes on radical content

One of the initial reports on the presence of persistent radicals in wood was published in 1960 by Rex,^[21] who used electron paramagnetic (or spin) resonance (EPR/ESR). Rex examined lignins, tannins, and humic acids found in plants and coal, and observed a distinct line of (6 ± 2) G at a g factor = 2.003 ± 0.002 in the EPR scans (the g factor or g value is a quantity that evaluates the ratio of magnetic moment and gyromagnetic moment of an atom and can provide useful information about the electronic structure of a paramagnetic center).^[22] This observation revealed the presence of an unprecedented stable radical.^[21] During this study, it was also discovered that the detected radicals were not present in native lignin in wood and, as such, they did not necessarily originate from simple aging or decomposition of wood. It was witnessed that the detected radical species were stable over a span of years in the air, and consequently, it was believed that they were formed when native lignin in wood was polymerized to lignin through acidic or fungal attack. Rex also attested that the stable radicals present in lignin were protected by their macroenvironment and able to live inside of lignin micelles through the process of “coalification” for tentatively 10^8 years. Coalification is a process in which peat deposits of root and bark undergo numerous physical and chemical changes through bacterial decay, compaction, heat, and aging.^[23] The process of coalification was believed to have a direct impact on the spin content in woods. To probe this discovery further, an EPR study on fresh and air-

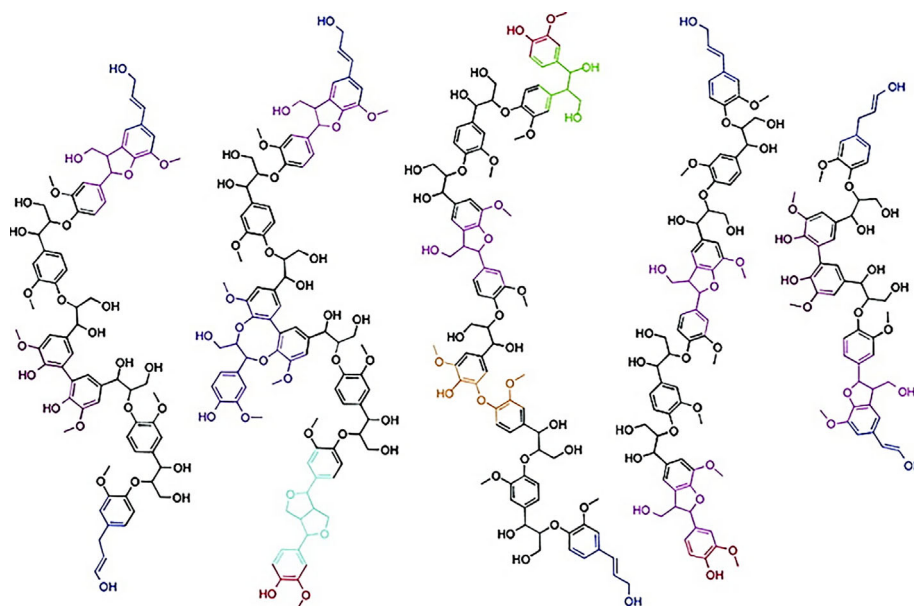


Figure 3. A recent constitutional scheme of oligomeric softwood milled wood lignin structure (reprinted with permission from the American Chemical Society, 2011).^[5]

dried wood-shavings samples from pine, oak, eucalyptus, redwood, and spruce was performed. The study showed low-spin concentrations ($< 10^{14}$ spins per gram (s g^{-1})), which indicated agreement with the discovery. Also, further extraction studies revealed that Soxhlet extractions of residual wood fractions by using carbon disulfide–ethanol–dioxane, respectively, led to the elimination of all free radicals detectable by EPR. Therefore, it was concluded that lignin was the polymerization product of compounds capable of reacting with semiquinone free radicals during hydrolytic and dehydrogenative degradation of plant tissues.^[21] These polymers, with their trapped free radicals, were believed to survive geochemical processes of degradation. It was also noted that various aromatic functional groups, such as $-\text{OH}$, $-\text{SH}$, and $-\text{NH}_2$ undergo the process of dehydrogenation to yield semiquinone radicals. Similarly, another report by Freudenberg indicated that lignin polymerization might originate from the process of dehydrogenation or oxidative deprotonation of phenolic species from coniferyl/sinapyl alcohol or hydrolysis of glycoside linkages.^[24] This study also specified that lignin polymerization followed a free radical mechanism that involved a semiquinone radical intermediate.^[24]

As anticipated, the research was further extended from the detection to the quantification of free radicals in lignin. One of the initial studies on the measurement of spin content on a variety of lignin samples was studied and published by Steelink et al.^[25] Their data strongly supported the presence of semiquinone-type radicals and diamagnetic quinhydrone moieties.^[25] All samples in these experiments (Table 1) showed unpaired spin contents. Native, Bjorkman and Klason lignin (Table 1, entries 1–3) showed the lowest spin concentrations, whereas alkali and fungal preparations (Table 1, entries 4–9) showed much greater spin concentrations. The last preparations were believed to have undergone demethylation, leading to the for-

Table 1. Radical content in various lignin samples. (Standard used for comparison: diphenylpicrylhydrazyl.)

Entry	Sample	[s g^{-1}]	Radical content	
			Estimated mol wt	[spin mol^{-1}]
1	Brauns native spruce	0.5×10^{17}	1000 ^[a]	5×10^{19}
2	Bjorkman spruce	1.0×10^{17}	11 000 ^[b]	1.1×10^{21}
3	Klason spruce	0.4×10^{17}	5000 ^[a]	1.5×10^{20}
4	Klason redwood	0.9×10^{17}	–	–
5	decayed western hemlock wood meal	0.9×10^{17}	–	–
6	kraft yellow pine (softwood kraft)	3.0×10^{17}	5000 ^[a]	1.5×10^{21}
7	kraft-treated native spruce	4.0×10^{17}	–	–
8	calcium lignin sulfonic acid	1.5×10^{17}	10 000 ^[a]	3.0×10^{21}
9	indulin AT (softwood kraft)	3.0×10^{17}	–	–

[a] From Ref. [28]. [b] From Ref. [29].

mation of *ortho*-quinoid or quinone methide groups, justifying greater stable spin contents relative to the native or acidic preparations.^[25–27]

The idea of spin counting was extended to samples of brown and white rot fungi to analyze wood decay as a function of time. This experiment showed a two- to threefold increase in spin content for both fungal samples over time. (Figure 4A,B). This data also revealed that decayed hardwood had the propensity to create greater spin concentrations than that of the decayed softwood species. An appropriate experimental model was designed to support these claims.^[30–31] The model predicted and substantiated that the quinoid functionalities in the presence of phenolic moieties were responsible for electron donor–acceptor complexes. These donor–acceptor complexes, such as quinhydrone, result in the formation of stable

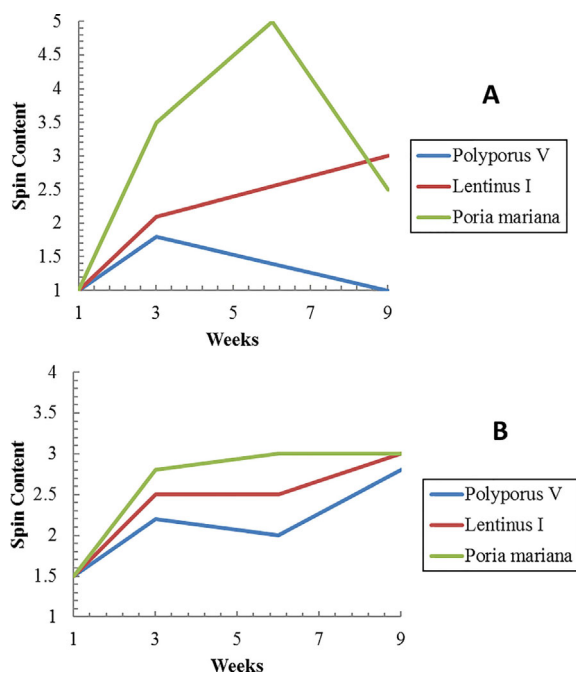
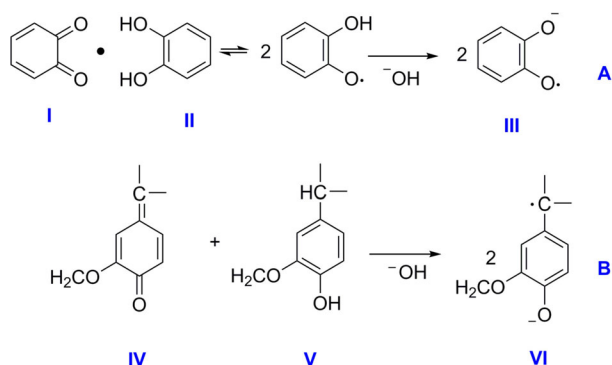


Figure 4. Radical contents in A) decayed sweet gum and B) decayed southern pine (modified and replotted with permission from the American Chemical Society, 1966).^[32]



Scheme 1. The generation of stable semiquinone radical anions under alkaline media.^[30,31]

radical anions (semiquinone anions) in alkaline media (Scheme 1).

The process of biological and chemical oxidation equally contributes to the generation of quinone species (Scheme 1, I), which eventually increases the contributions of reactions A and B. Alternatively, enzymatic and/or alkaline demethylation^[33] generates substituted catechols (Scheme 1, II, III), which could be easily oxidized to *ortho*-quinones. Alkaline demethylation also participates in the quinhydrone system (Scheme 1, IV, V, VI). In short, even negligible amounts of *ortho*- or *para*-benzoquinone species, in the presence of phenolic functional groups and under alkaline treatments, can justify the presence of radicals. Thus, it is not surprising that the residual spin is almost absent in neutral or acidic forms of lignin in whole wood and even native lignin, which shows only a small amount, as op-

posed to chemically modified lignins. This type of persistent radicals could be generated because of a small equilibrium concentration of I in equation A (Scheme 1), or from a semiquinone polymer matrix^[34,35] containing electron donor–acceptor groups, or radicals stabilized within the polymeric network.^[36,37]

Overall, these reports showed that the paramagnetism in lignin arose from even minuscule amounts of phenoxy radicals or oxidized products. The increase in radical centers upon an alkaline treatment arises from quinhydrone-type species (electron donor–acceptor). The spin content of both types of radicals significantly increases with the extent of decay (biological, chemical/oxidative) of the lignin, the nature of its precursors and the nature of its degradation products.

2.2. Effect of mechanical and chemical attack on radical content

Because it was evident that mechanical and chemical processes played a crucial role in radical formation in lignin, researchers also dedicated efforts towards exploring this hypothesis more. Many reports in the literature emphasized that not only the botanical origin and related natural processes, but the treatment and isolation of lignin contributed to the spin content in lignin. Data reported by Košíková et al. showed that prehydrolysis lignin (WL) and organosolv lignin (OL) contains 20×10^{15} and 30×10^{15} $s\ g^{-1}$, respectively (g factor at $g = 2.00$).^[38] Both of these samples showed a single line signal in the EPR spectra (Figure 5). These numbers were also found to be in agreement with those of mildly extracted lignins.^[38,39] Interest-

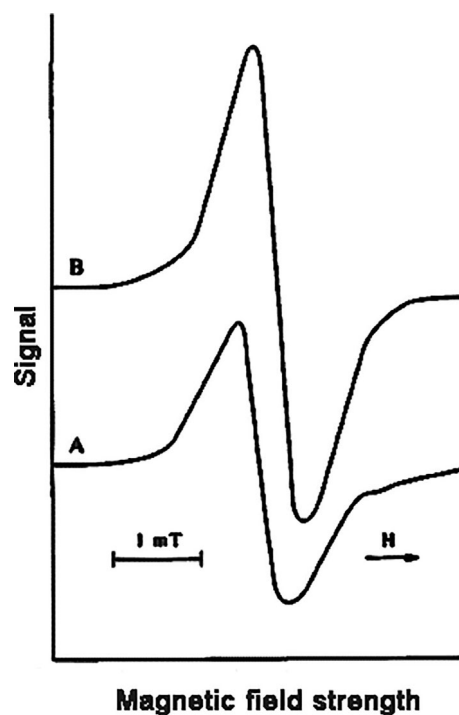


Figure 5. EPR spectra of lignin preparations by Kosikova et al.^[38] at 130 °C; A) beech wood lignin, and B) spruce OL (modified and revised with permission from Elsevier, 1993).

ingly, spruce lignin showed the presence of only $4 \times 10^{15} \text{ sg}^{-1}$ prior to isolation.^[32] This provides evidence that mechanical and chemical effects during lignin isolation are responsible for additional spins, possibly resulting from aryloxy- or semiquinone-type radicals. Moreover, based on the results by Kleinert, it was construed that differences between spin contents in lignins originated from their stabilizing capacity, which depended on the method of preparation.^[40]

In another experiment by Kleinert, air-dried wood from black spruce (*Pinea mariana*) and its kraft pulp were used to perform EPR measurements. In this study, mechanically undamaged wood (followed by grinding to filter it through a 40 mesh in a laboratory Wiley mill) was used after ball-milling (Figure 6).^[40]

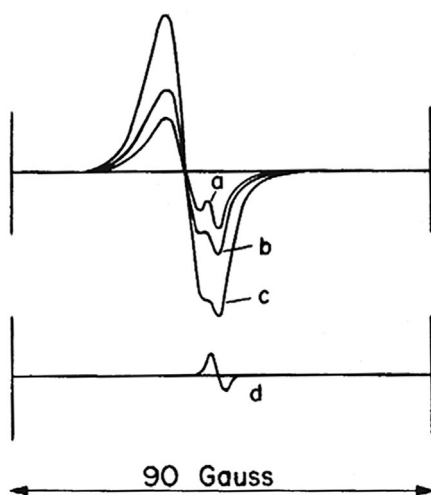
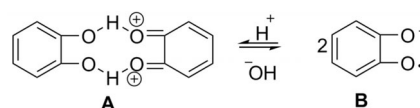


Figure 6. ESR signals of wood (*P. mariana*) in progressive stages of defibrillation: a) initial undamaged wood, b) wood ground through mesh 40 in a Wiley mill, c) wood after ball milling, d) high-purity bleached pulp. (Reprinted with permission from the American Chemical Society, 1963.)^[40]

For comparison, a sample of ball-milled, high purity, bleached pulp was used because it was known to show a small signal. It was observed that the radical content increased as the wood particle size decreased. Consequently, the reason for the greater wood signal than that of the pulp signal was perceived to be attributed to the branched and rigid structure of lignin, which was more resistant to grinding than that of cellulose. Kleinert also investigated ESR signals of two unbleached kraft pulps at increasing beating times by using a Valley beater. No significant differences in signals were observed by EPR. The study concluded that the mechanical defibrillation of fibers caused covalent bonds to rupture with the subsequent formation of macroradicals, along with a subsequent increase in specific surface.^[40] Upon drying, these macroradicals were responsible for the increase in interfiber bonding. This hypothesis also explained the superior strength of sheets formed from pulp that was never dried, compared with those previously dried. The uniform radical content detected in pulps beaten to reduce the Canadian Standard Freeness (CSF) was believed to relate to macroradicals being stabilized and trapped in residual lignin. This was supported by similar ESR signals present in the

initial wood and unbleached kraft pulp samples, but significantly different from signals received from isolated lignin.

Steelink et al. also studied the effect of conversion of lignin to its metal salts. In this study, a few lignin samples were converted into their metal salts (through the addition of ethanol and an aqueous solution of alkali). A 100-fold increase in spin content was observed. When these salts were acidified, the recovered product showed reversion to the original low-spin concentration. This experiment was also repeated under an inert atmosphere to observe the effect of molecular oxygen (ground-state oxygen, a diradical), but no significant changes were detected. This reversible change in radical concentration, which was facilitated by a change in pH alone, was assigned to the characteristics of quinhydrone-type systems (Scheme 2).^[25] Hardwood kraft lignins showed higher spin con-



Scheme 2. Reversible quinhydrone-type systems.^[25]

tents relative to those of softwoods. This confirmed that kraft treatment modified the lignin structure to promote radical formation when the pH was increased. Indeed, many reports unanimously agreed on the fact that hardwood lignin (containing high amounts of 3,5-dimethoxy-4-hydroxyphenyl groups) showed a higher spin content than that of the corresponding softwood lignin (which contains 3-methoxy-4-hydroxyphenyl elements as the primary constituent).^[41] The highest spin content was reported in alkali or soda lignin among the various samples. It was observed that the aerobic alkaline degradation of hardwood lignin produced 2,6-dimethoxyquinone, which quickly produced stable radical species.

Figure 7 shows some other semiquinone radical ion precursors (C–E), which are expected to generate quinhydrones and match with previously known lignin preparations

The quinhydrone model was further supported by reduction experiments with NaBH_4 . The reduction of carbonyl and quinoid groups with NaBH_4 revealed no significant effect on the lignin content. This behavior was explained by the equilibrium present between radical formation and destruction. However, the reduction conditions showed the ability of lignin to form

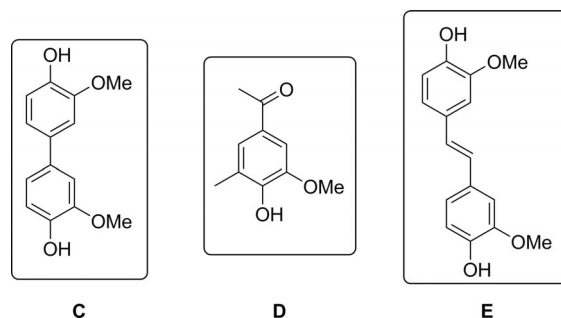


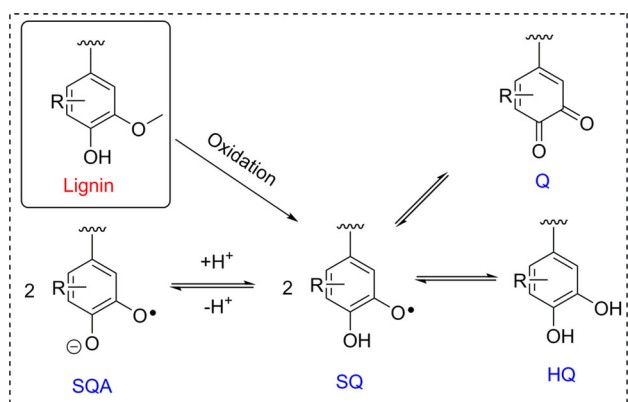
Figure 7. Precursors for semiquinone-type radicals.^[25]

Table 2. Spin content in lignin derivatives before and after various chemical modifications.

Entry	Sample	Spin content				
		Untreated ($\times 10^{17}$)	Na ^[a] /Ba ^[b] salt ($\times 10^{17}$)	Acidified salt ($\times 10^{17}$)	NaBH ₄ ($\times 10^{17}$)	Na salt of NaBH ₄ reduced ($\times 10^{17}$)
1	Brauns native spruce	0.5	50 ^[a]	0.5	1.1	8.4
2	Bjorkman spruce	1.0	15 ^[a]			
3	kraft yellow pine (softwood kraft)	3.0	100–300 ^[a]	3.0	1.3	22.0
4	kraft native spruce	4.0	70 ^[a]	–	–	–
5	indulin AT	3.0	72 ^[a]	–	–	–
6	hardwood kraft	8.0	550 ^[a] 880 ^[b]	–	–	–

[a] Data available with a sodium salt. [b] Data available with a barium salt.

radical anions, which are a prominent feature of the quinoid moiety (Table 2). The presence of semiquinone radicals stabilized within a polyphenolic matrix, such as lignin, was supported by three important observations.^[31,41,42] First, the lignin macromolecule had all of the necessary structural elements that promoted the generation of semiquinone-type radicals through oxidation reactions. Second, the radical content significantly increased when the pH was increased to alkaline conditions, which was elucidated by symproportionation reactions of hydroquinones and quinones to form semiquinones radicals and semiquinone anions (Scheme 3). These conclusions were believed to be true because the g factor (g_{iso}) of lignin was found to be similar to the g_{iso} factor observed with model semiquinone radicals.^[31,41,42]



Scheme 3. Formation of semiquinone radicals (SQ), hydroquinone (HQ) and a quinone (Q) leading from the semiquinone radical anion (SQA; R=OMe for syringyl subunits and R=H for guaiacyl subunits).^[43]

Steelink et al. converted native and kraft lignin into its salt form and found the concentration of the semiquinone radical ion to be 0.0017 radical OMe (0.01 spin molecule⁻¹) for native lignin and 0.003–0.01 radical OMe (0.08–0.25 spin molecule⁻¹) for kraft lignin.^[25] These numbers were in agreement with the numbers obtained for model compounds by Matsunaga.^[44] Marton and Adler detected as little as 0.01 carbonyl/OMe content by using UV spectrophotometry;^[45] this was higher than that of Steelink's number for quinoid carbonyl content. This comparison also highlighted the accuracy of the ESR method

for radical determination, relative to that of UV spectrophotometry, and confirmed that it was sensitive to even minor structural contributions.

In summary, all of these reports point toward the unanimous conclusion that many new radical centers are introduced upon alkali treatment, which indicates the presence of quinhydrone systems.

2.3. Effect of temperature on radical content

The next parameter that was examined for its effect on the spin content of lignin was temperature. Temperature is believed to play a significant role in the formation of radicals in lignin. The radical content in lignins decreased with increasing temperature (Figure 8). A report by Hatakeyama and Nakano supported these statements by showing a decline in radicals due to molecular vibrations occurring during heating of milled wood lignin (WL) and organosolv lignin (OL).^[46] However, this inversely proportional relationship was only applicable to certain types of lignin. The radical content in oxidized organosolv lignin (OOL) did not change when the temperature was varied from ambient temperature to 100 °C, whereas the radical content increased when the temperature was increased up to

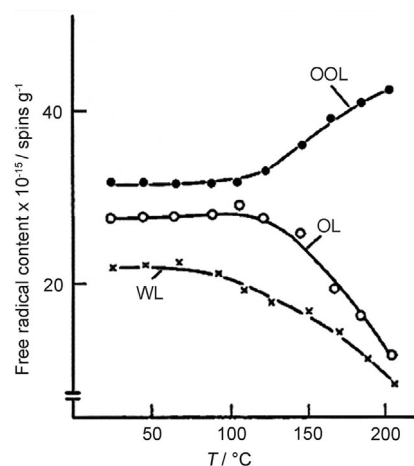


Figure 8. Effect of temperature on radicals before (OL, WL) and after oxidation (OOL)^[46] (reprinted and modified with permission from Elsevier, Copyright, 1993).

200 °C. Similar behavior was observed for dioxane lignin and thiolignin.^[46] This behavior was attributed to the process of thermal decomposition overcoming radical decay by molecular vibrations and, as a result, the radical content was seen to increase upon heating in the following order: OOL > OL > WL.^[46]

The observed increase in radicals in the case of OOL was attributed to the formation of benzoquinone structures.^[47] Two types of benzoquinone signals were detected in ESR investigations: 2,6-dimethoxy-*p*-benzosemiquinone radical and 5-hydroxy-2-methoxy-*p*-benzosemiquinone radical.^[48] The formation of these radicals was proposed to occur through an oxidative cleavage processes of syringyl (S type) and guaiacyl (G type) end groups in lignin. Although many mechanisms were proposed to explain these reactions, a common deduction was based on the hypothesis that the C α and C β carbon atoms of the S or G units performed a crucial role in commencing the formation of radicals.^[49] This was further investigated by monitoring the spin contents (by using ESR) for enzyme lignin from reed that was subjected to acidolysis and/or reduction reactions. This investigation indicated that the 5-hydroxy-2-methoxy-*p*-benzosemiquinone radical was a product of deprotonation of 6-hydroxy-2-methoxy-*p*-benzosemiquinone and was formed from syringyl end groups.

A similar trend was observed by Kleinert and Morton in an experiment conducted on alkaline pulp by using an in situ ESR technique.^[50] This study detected strong signals at the pulping temperature, which confirmed the formation of radical centers. A kinetic investigation of the alkaline delignification of wood also indicated the involvement of radical species.^[50] It was thus deduced that the alkaline conditions used during the pulping of wood, lignin, and carbohydrates actually promoted the degradation process by forming more radical centers. These macroradicals were believed to undergo various secondary reactions due to their high reactivity.

2.4. Photochemically produced quinoid structures in wood

It is thus far evident that the degradation of wood is triggered by various biological and chemical factors, such as white rot fungi, alkaline sulfite, or photochemical reactions, leading to a decrease in the methoxy content of lignin. A report by Leary in 1968 presented data that showed the effects of irradiation on glass-covered newspaper (made from *Pinus radiata*) by using a 1 kW carbon arc for 1000 h.^[51] A prominent loss (ca. 0.3%) in the amount of methoxy groups was observed. Experimental evidence suggested the presence of quinoid intermediates species formed during photo-oxidation, possibly *o*-quinone, *p*-quinone, or *p*-quinone methides. The possibility of *p*-quinone was omitted due to the absence of atmospheric oxygen during the experiments. It was speculated that the precautions of excluding oxygen stopped yellowing, and the wood retained its original methoxy content.^[51] This phenomenon was attributed to the hypothesis that wood yellowing was a photo-oxidative process and involved the formation of *p*-benzoquinones. The most prominent evidence for the photochemical production of quinoid structures in wood derived from a study in which the free phenolic hydroxyl groups were

masked with acetyl or methyl groups. Wood, which was acetylated, followed by immersion in an aqueous solution of NaOH (1 N) and acetic anhydride, yellowed slowly and did not show loss of methoxy groups when irradiated by light. Similar results were observed with the use of trace amounts of perchloric acid, leading to bleaching instead of yellowing under irradiation conditions. These findings indicated that lignin readily underwent oxidative demethoxylation and yellowing when it contained free phenolic hydroxyl groups. Because similar considerations governed the formation of quinones and quinone methides, it was speculated that they formed at the same stage when wood yellowed. These species, which are highly photoreactive themselves, were believed to degrade further, and thus, were not responsible for the final yellow color of the wood. This concurred with attempts to remove them from irradiated wood by reductive chemistry. Whereas an aqueous solution of NaBH₄ removed the yellow color effectively, hot stannous chloride showed no effect and hot sodium dithionite was only partially effective.

3. Methods of Spin Detection

3.1. Electron Paramagnetic Resonance (EPR)

Among the most efficient techniques for the detection of paramagnetism in matter is EPR (or ESR) spectroscopy with applications to the detection of radicals in lignin and biomass. For example, one of the early accounts available on this topic was a report on the detection of stable radicals in two straw samples: fresh straw and a straw that was immersed in water for six months.^[52] A rudimentary and rapid method of X-band EPR spectroscopy was used to quickly scan these samples for free radicals (Table 3 and Figure 9). The results showed a distinctive single broad signal that indicated the presence of stable free radicals. Although preliminary screening of radicals was performed by using X-band ESR, to further resolve the signal, high-resolution Q-band EPR spectroscopy was used.

The tentative nature of the radical structure from the signals of Q-band ESR spectroscopy was confirmed due to observed power saturation in the 10–20 dB range.^[52] The Q-band EPR signals were more informative than the X-band signals for de-

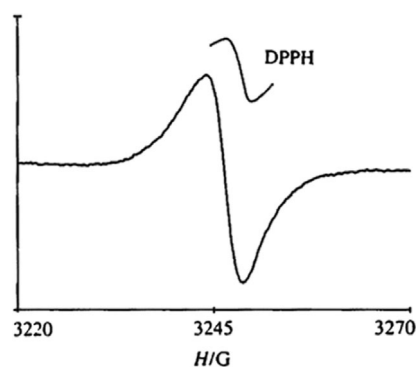
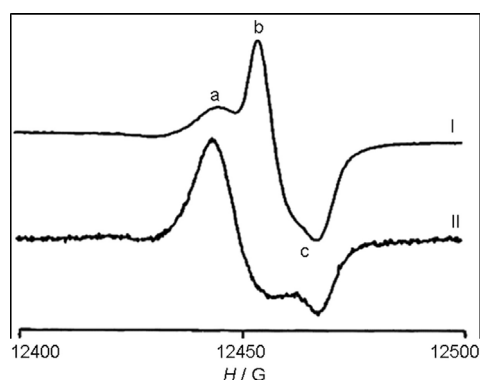


Figure 9. Representation of the X-band EPR signal from pond-rotted straw (reprinted with permission from Springer, Copyright, 1996).^[52] (Measured at 9.1 GHz; Table 3, sample 4; internal standard = DPPH.)

Table 3. X-band EPR data recorded for various straw samples.^[52]

Entry	Sample	Method of sample preparation	$G^{[a]}$
1	unrotted fresh straw	barn-stored straw stored at RT	2.0048
2	tank-rotted straw	straw soaked (6 months), sample removed, soaked in algal culture medium (2 weeks), RT	2.0037
3	repeat of entry 2 after further drying	as for entry 2, but with air-dried straw (7 days)	2.0046
4	pond-rotted straw	straw soaked in a pond (2 months), removed, and soaked in the same pond water (2 weeks), RT	2.0041
5	alkali-treated unrotted straw	unrotted straw (entry 1) immersed in 1 M NaOH overnight	NA ^[b]
6	soluble lignin recovered from aqueous solution containing entry 2	soluble lignin from aqueous solution containing entry 2 (precipitate from the algal culture in which sample 2 was soaked)	2.0041
7	soluble lignin recovered from aqueous solution containing entry 4	soluble lignin from aqueous solution containing entry 4 (precipitate from pond water in which entry 4 was soaked)	2.0047

[a] The g values are calculated relative to the g value for diphenylpicrylhydrazine (DPPH). [b] NA = not applicable.

**Figure 10.** Signal from Q-band EPR: I) unrotted straw and II) pond-rotted straw. (Reprinted with permission from Springer, Copyright, 1996.)^[52] Note: a, b, and c indicate specific signal intensities' maxima and minima.

ducing information regarding the nature of radicals. For example, Q-band EPR was used to distinguish various types of radical signals with different intensities from the same sample (Figure 10). Two major signals were detected from a fresh straw sample: one with a g value of 2.0046 (Figure 10, signal a) and another with greater intensity at a g value of 2.0019 (Figure 10, signal c). Along with these signals, which were observed in rotten straw samples, another signal with a g value of 2.0033 (Figure 10, signal b) was also detected. The most intense signals with similar g values and intensity were detected in pond rotten straw and fresh straw, but the signal for an unrotted sample showed the presence of intermediate g value signal (Figure 10, signal b).^[52] Based on these outcomes, it was speculated that signal b in Figure 10 and signals a and c had origins belonging to different radical sites.

Bährle et al. used X-band and high-field EPR techniques to investigate the spin content and g factors of radicals in various lignin samples.^[43] They used four samples from hardwood (beech and poplar) and softwood (pine and spruce) trees, which were used as raw materials for extraction experiments. Using various extraction techniques, the group prepared Klason, dioxane, and organosolv lignin and studied them against untreated wood samples. As anticipated, the lowest spin content was found to be in untreated wood samples (mean concentration $\approx 6 \times 10^{16}$ spins g^{-1} ; calculated for lignin fractions $\approx 1 \times 10^{17}$ to $\approx 5 \times 10^{17}$ spins g^{-1} ; Table 4). Within ex-

Table 4. Calculated g factors for various lignin preparations by using X-band EPR (at 9 GHz).^[43]

Entry	Sample	g factor
1	untreated wood	2.0049
2	Klason lignin	2.0039
3	dioxane lignin	2.0043
4	OL	2.0037

perimental error, these numbers were similar to those of the observed spin concentrations for the Klason and dioxane lignins ($\approx 1.7 \times 10^{17}$ and 2.1×10^{17} spins g^{-1} , respectively). Therefore, it was concluded that these two methods did not largely affect radical concentrations. On the contrary, OL showed a dramatic 10-fold increase in radical concentration ($\approx 1.9 \times 10^{18}$ spins g^{-1}). The trigger for this was assumed to be the higher temperature (200 °C) of the organosolv process than that of the lower temperatures in Klason (100 °C) and dioxane (90 °C) processes. Thus, this was credited to be the phenomenon that 200 °C was the optimum temperature required for homolytic bond cleavage that led to the formation of additional radicals.

Although the highest g factor was observed for untreated wood, there was no correlation found between radical content and g factors. Additionally, it was observed that the g factors of these radicals mainly depended on the process of extraction and pH of the solution during extraction and not their biological origin. This behavior was analyzed by using high-field EPR spectroscopy (263 GHz). This high-field technique, coupled with high resolution, was also used for detecting radical species in lignin. The radical species were identified as *o*-semiquinone radicals and believed to be present in various protonation states, such as SH3⁺, SH2, SH1⁻, and S2⁻ (Figure 11 A). DFT calculations agreed with these conclusions, and the g values of the proposed structures were in rational agreement with the experimental data.

Predominantly, the variation in g factors was attributed to pH values of the solution during extractions. The pH was believed to influence the protonation states of semiquinones that eventually led to additional radical species. To probe whether the additional radicals in OL were different from the radicals in Klason and dioxane lignins, X-band EPR (Figure 11 C)

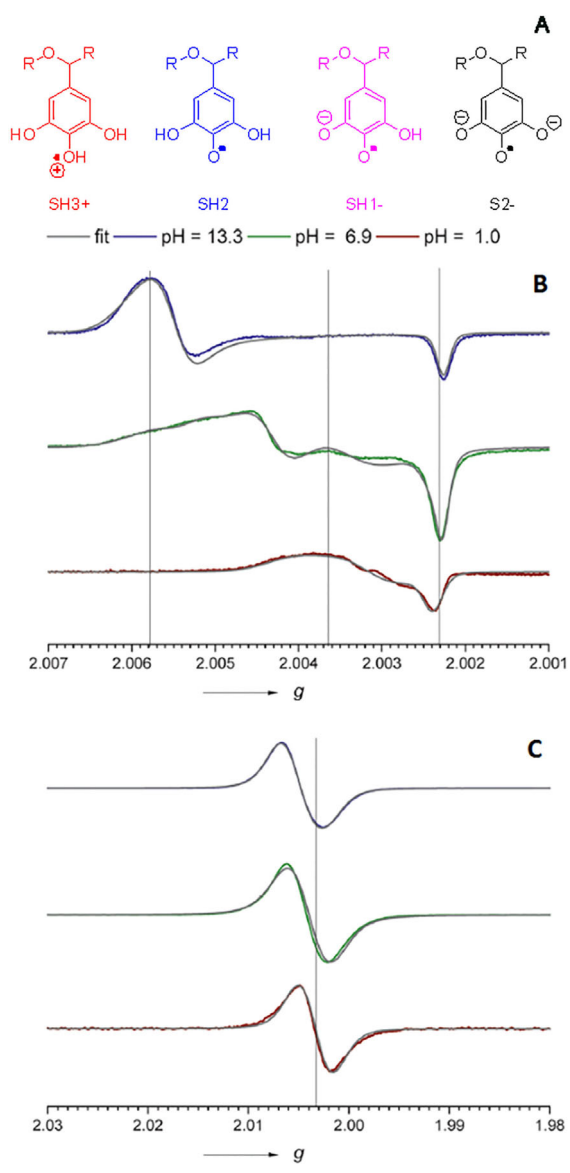


Figure 11. A) Structures of the proposed radical species (SH3+, SH2, SH1-, and S2-). B) High-field EPR spectra of Klason lignin at pH 1.0, 6.9, and 13.3. C) X-band EPR spectra of the pine Klason lignin sample at pH 1.0, 6.9, and 13.3. R = CH₃ was used for all DFT calculations. (Reprinted with permission from the American Chemical Society, Copyright, 2015.)^[43]

and high-field EPR (Figure 11 B) analyses were performed on such lignins at varying pH values.^[43]

The technique of high-field EPR was especially attractive in this case. From the data collected, it was revealed that not only the neutral form SH2 was dominant at pH 3.7–8.9, but SH3+, SH1-, and S2- species were also detectable at those pH values (Figure 11 A).^[43] On the other hand, the deprotonated species (SH1- and S2-) were dominant only at pH 13. DFT calculations concurred with this experimental model. To test if similar species were present in lignin extracted by different methods, high-field EPR spectra for each were also recorded (Figure 12).^[43] Hardwood, softwood OL, and Klason samples showed identical *g* values. Furthermore, it was concluded that

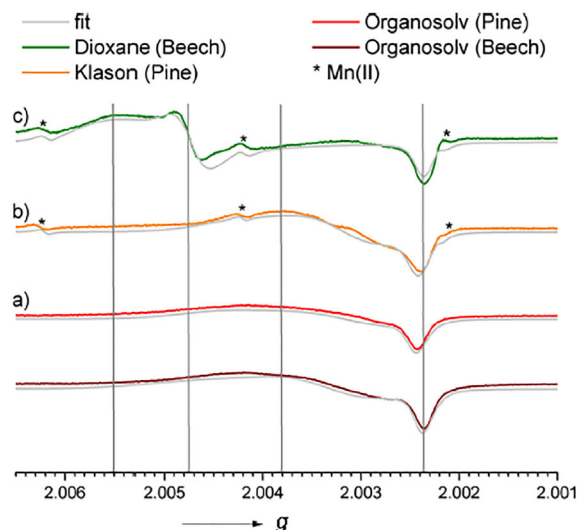


Figure 12. High-field EPR spectra of a) hardwood (beech) and softwood (pine) OL, b) softwood (pine) Klason lignin, and c) hardwood (beech) dioxane lignin. Asterisk indicates traces of Mn^{II}. (Reprinted with permission from the American Chemical Society, Copyright, 2015.)^[43]

the dominant radical species in OL and Klason lignin was the SH3+ species because the *g* values tentatively matched with the radical species in Figure 11 C (at pH 1). For the dioxane lignin, the SH2 radical was the dominant species (Figure 11 C, at pH 13.3).^[43] These observations supported the hypothesis that the pH value during the extraction method was accountable for the differences in the EPR spectra of lignin samples.

3.2. EPR for radicals in wood, carbonaceous solids, and pulp

EPR spectroscopy is not only useful for the elucidation of lignin radicals, but also for examining radicals in similar biomaterials, such as carbonaceous solids (e.g., coal tar). Pulsed EPR spectroscopy is especially useful in studying radical structures in coal and reaction mechanisms involved in coal tar pitch (CTP).^[53,54] The ¹H and ¹³C hyperfine spectra of coal were recorded by means of hyperfine sublevel correlation (HYSCORE) spectroscopy by the group of Ikoma.^[55] Their work revealed that the majority of coal radicals were delocalized over more than seven aromatic rings. This finding was also indicative of dehydrogenative polymerization in I₂-treated CTP.^[55–57]

ESR spectroscopy is also an established method for pulp analysis during bleaching processes. ESR spectroscopy allowed the detection of both organic radical species: lignin and carbohydrate radicals. The evolution of lignin-based radicals was determined through observing lignin radical intensity during bleaching of pulp and it was concluded that a small amount of lignin was left at the end of the process.^[58] This method was also useful in fine bleaching and yellowing studies. During these investigations, it was confirmed that new organic radicals were generated on carbohydrates during kraft pulping, especially in cellulose. This finding was in agreement with the statements made earlier regarding the generation of new radicals upon chemical treatments of these biomaterials.^[25,41] The

ESR method is also very helpful for the detection of metal ions in pulp at very low concentrations through the detection of strong and stable metal-ion complexes with pulp components.^[59,60]

A study performed by Brai et al. involved an investigation of wood samples by ESR spectroscopy to elucidate their radical structures and concentrations.^[61] In this study, researchers observed distinct differences between hardwood and softwood samples. It is acknowledged that the hardwood cellular structure is more complex than that of softwood and can vary significantly among different species. The EPR study showed a larger a parameter ($a = \Delta B_L / \Delta B_G$), which measures the degree of homogeneity of line broadening. Hardwood was characterized by smaller spin-spin relaxation times than those of softwood. This behavior was assumed to originate from differences in their microscopic structures.^[61]

X- and D-band ESR spectroscopy were useful in the detection of free radicals formed during radio- and photolysis of lignocellulosic compounds. Kuzina et al. reported that, upon γ and UV irradiation of wood, a singlet signal due to radicals with carbon-carbon conjugated systems was apparent.^[62] This was a preliminary report that showed the determination of radiation, chemical, and quantum yields of radical formation in lignin and wood. Also, the formation of formyl and peroxide radicals in irradiated wood were detected by ESR spectroscopy.^[62]

3.2.1. EPR techniques for lignin pyrolysis and associated radical species at low temperature

Other EPR techniques used in lignin chemistry include low- (LTMI-EPR) and high- temperature matrix isolation EPR (HTMI-EPR), owing to their application in the pyrolytic degradation of lignin and associated radical intermediates. The reactions involved in pyrolysis of lignin are known to be extremely complex. Therefore, techniques that allow the study of various radical intermediates at high temperatures and the corresponding products are of extreme value. This section aims to concisely summarize recent EPR reports dealing with lignin pyrolysis and the detection of related radical species and corresponding molecular products.

A recent study performed on lignin pyrolysis at 450 °C, in which the radical intermediates were analyzed by using the LTMI-EPR technique, revealed interesting findings.^[63] Kibet et al. used partial and conventional pyrolysis; in partial pyrolysis, the same lignin sample was pyrolyzed at selected temperatures, whereas in conventional pyrolysis various lignin samples were pyrolyzed at each of their pyrolysis temperatures. The results of partial pyrolysis showed that the products were mostly observed between 300 and 500 °C, whereas for conventional pyrolysis the products were observed between 400 and 500 °C. A representative spectrum of trapped radicals is depicted in Figure 13 (spectrum 1). The spectrum was a singlet with $g = 2.0072$ and spectral line width (ΔH_{p-p}) of 14.0 G. Minor signals on both sides of the main spectrum (marked with an asterisk in Figure 13A) originated from the presence of trace quantities

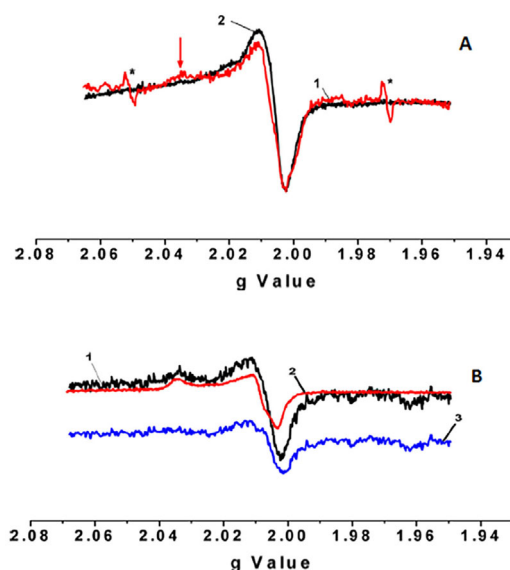


Figure 13. A) EPR spectra of free radicals from lignin (spectrum 1: $g = 2.0071$, $\Delta H_{p-p} = 13.5$ G, 450 °C) and tobacco pyrolysis (spectrum 2: $g = 2.0056$, $\Delta H_{p-p} = 13$ G, at 450 °C). B) EPR spectra of radicals from lignin pyrolysis and 0.1 torr (= 133.322 Pa) air (black line; $g = 2.0073$, $\Delta H_{p-p} = 15.0$ G, at 450 °C) and the overlaid reference EPR spectrum of radicals (red; $g = 2.0089$) from heating of tobacco (450 °C in vacuum). The blue spectrum ($g = 2.0064$, $\Delta H_{p-p} = 18$ G) shows the subtraction spectrum of the lignin and radicals. (Reprinted with permission from the American Chemical Society, Copyright 2012.)^[63]

of oxygen as E lines ($K = 1$, $J = 2$, $M = 1 \rightarrow 2$); it was believed that these could be easily removed by annealing.^[64,65]

An EPR spectrum from a Burley tobacco sample was compared with a lignin sample because the pyrolysis of tobacco was similar to that of the pyrolysis of lignin (Figure 13A, spectrum 2).^[66,67] These similarities originated from radicals formed, such as catechol, hydroquinone, and other organics, in the presence of trace quantities of oxygen.^[65,68–71] If the spectrum of tobacco (Figure 13, spectrum 2, black line) was subtracted from the spectrum of EPR radicals from the lignin pyrolysis (Figure 13, spectrum 1, red line), the resulting subtraction spectrum was obtained with an elevated g value of 2.0064 and $\Delta H_{p-p} = 18$ G (Figure 13, spectrum 3, blue line). This change in the spectrum closely matched that of a phenoxy or substituted phenoxy, such as a hydroxyphenoxy (semiquinone radical).^[72] The radicals from phenol and hydroquinone/catechol pyrolysis (and photolysis) were generated from lignin degradation, previously identified as phenoxy and semiquinone radicals, respectively.^[71,73–75] The phenoxy radical spectrum showed a broad spectral line width ($\Delta H_{p-p} = 16$ G), whereas the semiquinone radical showed a narrower line width ($\Delta H_{p-p} = 12$ G), possibly due to phenoxy linkages, which were present at higher concentration than those of semiquinones in lignin pyrolysis.^[65,76] Consequently, from these results, it was concluded that the free radical species were mostly created from phenolic linkages in lignin and were possible precursors to the formation of phenolic compounds, such as 2,6-dimethoxyphenoxy (syringyl groups), 2-methoxyphenoxy (guaiacyl groups), and

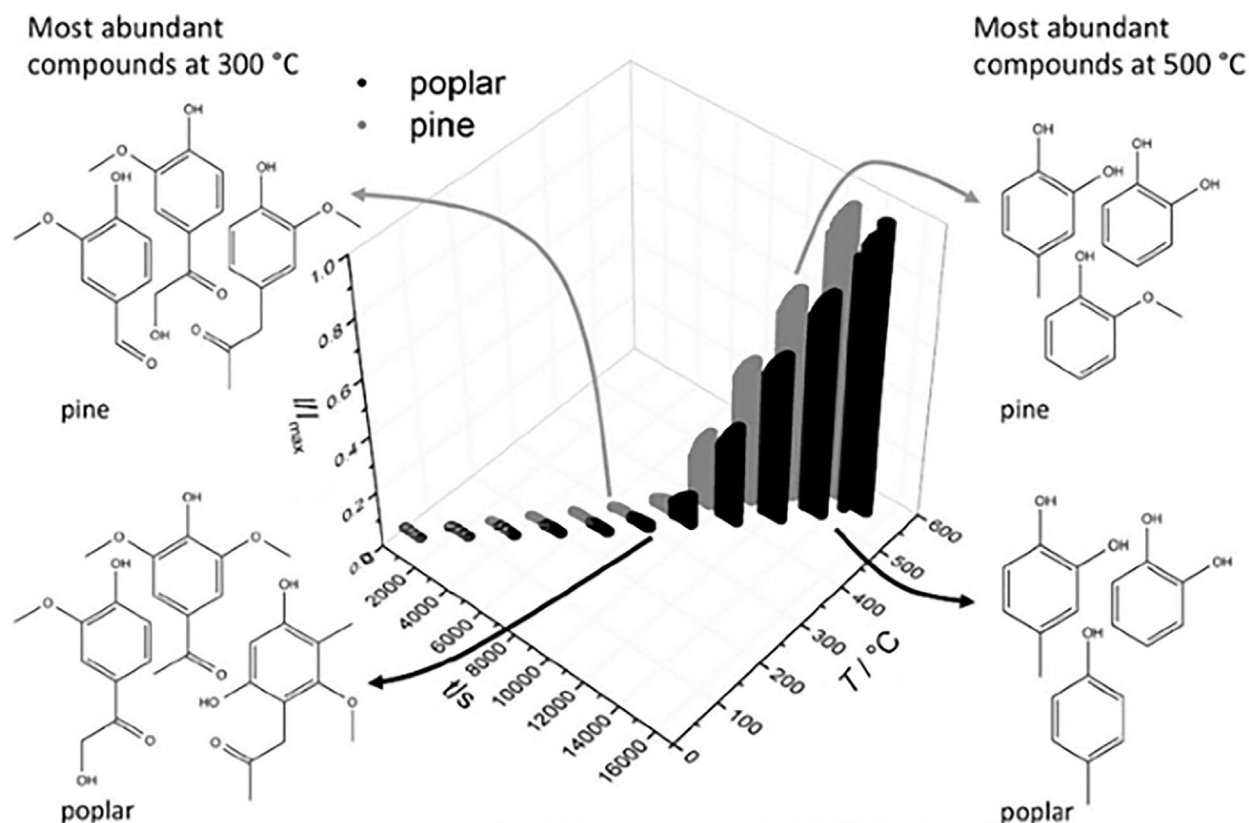


Figure 14. The standardized spin content of poplar and pine Klason lignin during pyrolysis. (Reprinted with permission from Wiley, Copyright, 2014.)^[77]

phenols for (phenoxy groups). GC-MS analyses also supported these conclusions.

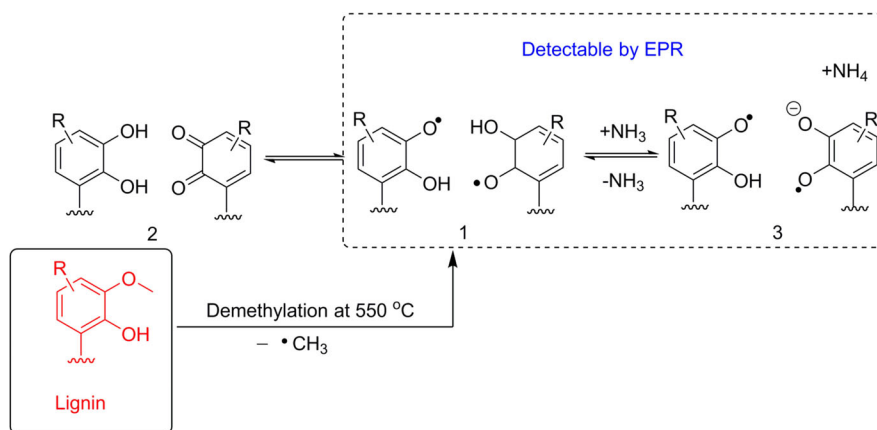
Overall, phenolic compounds marked their dominance in lignin pyrolysis and all major products, such as catechol, syringol (2,6-dimethoxyphenol), phenol, and guaiacol (2-methoxyphenol), constituted more than 40% of the total product formation.^[63] The structures of reaction intermediates were analyzed by using a LTMI-EPR instrument attached to a pyrolysis reactor. This technique was used to observe important radical precursors, such as methoxy, phenoxy, and substituted phenoxy. These radical precursors were believed to lead to the formation of many phenolic products, such as phenols, phenol derivatives, syringol, and guaiacol.^[63]

3.2.2. EPR techniques for lignin pyrolysis and associated radical species at high temperatures

It is clear that temperature plays a crucial part in defining the origin of these radical species during pyrolysis. Subsequently, it is important to comprehend the exact range of temperature that has the highest impact on the cleavage of bonds possibly leading to such radical species. Hence, similar to the technique discussed in Section 3.1.1, in situ high-temperature EPR has also been used to study the formation of semiquinone radicals during pyrolysis at very high temperatures and to identify those radical intermediates involved.^[77] Also, in situ EPR techniques have been used to study the pathway of radical formation during the pyrolysis of hardwood and softwood Klason

lignins, and its impact on the final products. A dynamic pyrolysis experiment was performed to determine the exact temperature at which radical depolymerization occurred. In this experiment, two Klason lignin samples (poplar and pine) were heated gradually from 50 to 550 °C and their radical content was determined at various temperatures (Figure 14). The accumulated data indicated that the radical concentration remained at a constant low value up to about 300 °C. However, beyond this temperature, the radical content was seen to dramatically increase. The highest increase in radical concentration was observed between 350 and 400 °C.

Similarly, pyrolysis GC-MS analyses were useful in the detection of stable volatile products under identical conditions to those of the EPR experiments. This product formation was believed to lead to the following general conclusions that could be applied to any lignin samples. The formation of three main types of final products was apparent: 1) alkoxy-substituted phenols with an aliphatic substituent with a keto group at the α position, 2) degraded products that lost their alkylketo substituent with one or more alkoxy substituents, and 3) phenols containing small aliphatic substituents and hydroxyl groups. The quantity of phenol alkoxy ketones (product group 1) in the volatile fraction gradually increased with temperature up to 350 °C, but further elevation in temperature and radical concentration resulted in a steady decline in product group 1, whereas the amount of alkoxy phenols (group 2) increased up to 450 °C. After further temperature elevation (500 and 550 °C), more radicals were observed and detected as



Scheme 4. Pathway for the generation and successive reactions of semiquinone radicals (recreated with permission from Wiley, Copyright, 2014).^[77]

phenolic compounds from product group 3. Hardwood and softwood lignins showed distinct differences: although phenol alkoxy ketones (product group 2) dominated at 300 and 350 °C, softwood showed a lower selectivity. At 550 °C, the amount of phenolic compounds (group 3) decreased. Although softwood lignin phenols dominated the overall product formation, hardwood lignin pyrolysis produced high-molecular-weight products. Because hardwood lignin contains a large amount of syringyl subunits, pyrolysis yielded a significant amount of phenolic compounds with two methoxy substituents, such as 2,6-dimethoxyphenol and 4-hydroxy-3,5-dimethoxybenzaldehyde. The guaiacyl subunit in softwood formed mostly phenolic compounds, such as vanillin and guaiacol.

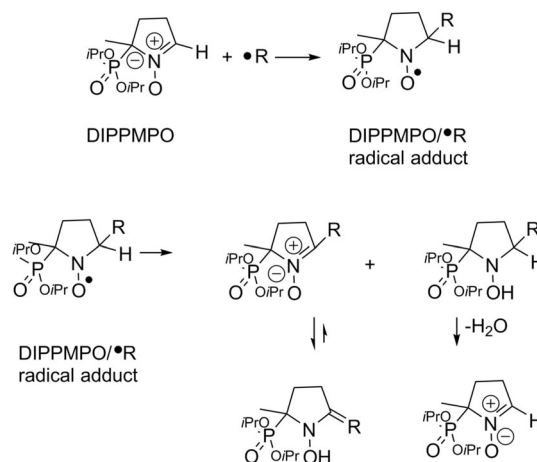
It was clear from the investigations that the pyrolytic residue of hardwood lignin showed a dramatic increase in signal intensity compared with that of softwood lignin. The equilibrium for the disproportionation reaction (Scheme 4) of two semiquinone radicals (1) to a quinone and a hydroquinone (2) was towards the side of radicals and radical anions (1 and 3), especially after the addition of ammonia. This explains the increase in EPR signal intensity because the addition of ammonia was proportional to the concentration of quinone and hydroquinone units in lignin. The addition of ammonia also explained why hardwood lignin had a higher signal intensity than that of softwoods (after ammonia exposure) because the concentrations of quinone- and hydroquinone-like species were higher in hardwood lignins. This also reinforced the suggested radical disproportionation mechanism.

3.3. ³¹P NMR spectroscopy for the detection of free radicals

The technique of spin trapping has been used in conjunction with ³¹P NMR spectroscopy for effective qualitative and quantitative analyses of radical species to provide a viable alternative to EPR. Although this technique has not been directly used to detect stable organic radicals in lignin, it has been particularly useful for the study of relevant transformations.^[78]

The primary difference between EPR and ³¹P NMR spectroscopy techniques is that EPR relies more on product analysis to determine the structure of reactive intermediates, whereas

³¹P NMR spectroscopy helps with the formation of direct stable adducts. A spin trap containing a phosphorous label plays a key role in making these adducts. For example, it has been reported that free radicals in lignin model compounds react with a nitroxide phosphorous compound, 5-diisopropoxyphosphoryl-5-methyl-1-pyrroline-*N*-oxide (DIPPMPO) and form stable adducts. These adducts are then detected and quantified by means of ³¹P NMR spectroscopy.^[79] The mechanistic pathway for spin trapping of such radicals (R) by using the spin trap DIPPMPO is depicted in Scheme 5.^[79] The ³¹P NMR spectroscopic technique has been established and utilized to assign signals for radical adducts originating from oxygen- and carbon-centered species in various model compounds. The chemical shifts for hydroxyl and superoxide were observed at $\delta = 25.3$ ppm and $\delta = 16.9$ and 17.1 ppm (in phosphate buffer), respectively. The same method was also applied for the detection of phenoxy^[80] ($\delta = 25.2$ ppm) and ketyl radicals.^[81] This method is particularly useful to study the photochemistry of lignin model compounds and reaction mechanisms.^[82] In summary, DIPPMPO as a spin trap provides an excellent way to identify free radical intermediates.



Scheme 5. The mechanism for spin trapping of radical R (from model compounds) by using DIPPMPO.^[79-81]

4. Spin-Trapping ESR Studies of Unstable Radicals from Lignin

So far, we have reviewed the use of ESR in determining the nature and concentration of radicals. ESR is also used for trapping and studying trapped radicals. The ESR technique, combined with spin trapping, is one of the most suitable and widely used techniques for assessing the formation of free radical intermediates in biological systems, and it has been effectively applied in various biological systems. Among various spin traps used, nitroxyl or nitron radicals are unanimously popular and the most accepted spin traps (e.g., cyclic 5-(diethoxyphosphoryl)-5-methyl-1-pyrroline-*N*-oxide (DEPMPO),^[83,84] 5,5-dimethyl-1-pyrroline *N*-oxide (DMPO))^[85] because of their stability due to the delocalization of spin over the N–O bond. These traps produce distinct and characteristic spin adducts with O₂ and OH radicals.^[86] In particular, reactions of hydroxyl, carbon-centered, or hydroperoxide radicals with nitrones produce very stable nitron-radical spin adducts. The lifetime of these spin-trap adducts was observed to be short (≈ 45 min), although considerably longer than the lifetime of naturally occurring radicals in UV-irradiated wood. EPR is a popular method for detection, but has not been widely used to characterize photoinduced radicals in wood.^[87,88] Among few initial studies, Humar et al. reported a method for the in situ inspection and characterization of radicals during the photodegradation of wood by using a spin trap.^[89]

This study showed some interesting results regarding radicals involved in photodegradation. In this study, the EPR signal for carbon-centered radical adducts was found to be most abundant (> 58%) during the photodegradation of wood. The next most abundant radical adduct was found to be the hydroxyl radical–DEPMPO adduct (35%), whereas hydroperoxide radical adduct species were only about 6% (Table 5 and Figure 15). These observations supported the previously reported hypothesis that carbon-centered radicals were more stable than the hydroxyl ones due to better stabilization of radical species.^[90] Humar et al. also reported the absence of free radicals in wood that was not exposed to UV light.^[89] This may be justified by the fact that wood stored in dark and dry places for a long time contained negligible amounts of intrinsic free radicals.

This was further supported by additional experiments. A significant difference was witnessed in the respective concentra-

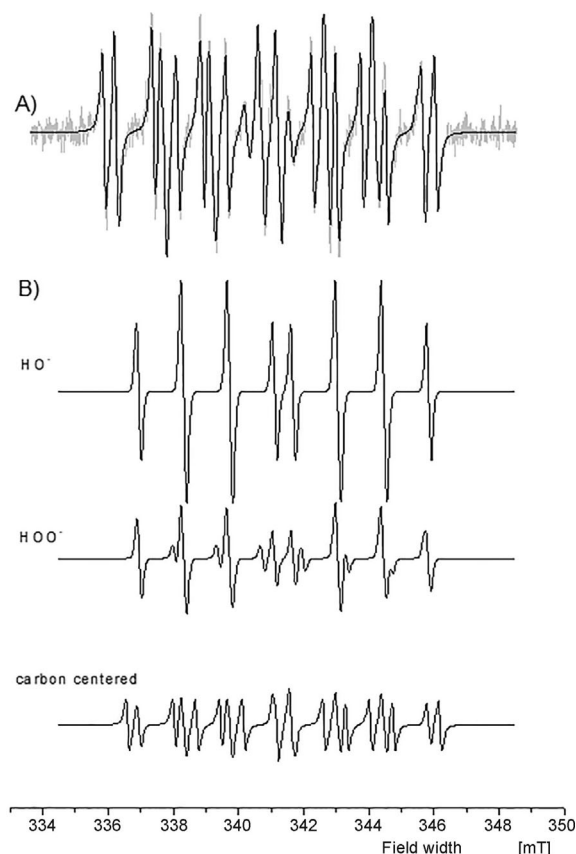


Figure 15. EPR spectra of DEPMPO radical adducts in wood (1 h irradiation, UV light at $\lambda = 280$ nm). A) Experimental spectrum (a thin gray line) merged with simulated EPR spectrum (a thick black line). B) The best fit through a superposition of the spectral components of DEPMPO adducts from OH^\cdot , HOO^\cdot , and -C^\cdot radicals.^[89] (Reprinted and adapted with permission from OCLC, Copyright, 2001–2016)

tions of stable radical adducts in photodegraded BRW and cellulose from those in photodegraded wood.^[89] The major difference was observed between BRW and wood in the ratio of carbon-centered radical adducts to hydroperoxide radical adducts. Although the respective concentrations of carbon-centered radical adducts were higher than those in BRW (58 and 38%, respectively), the relative concentration of hydroperoxide radical adducts increased from about 6% in wood to 38% in BRW (Table 5 and Figure 16). The amount of hydroxyl radical adducts in cellulose was about 49%; that of hydroperoxide about 16%. The relative amount of carbon-centered radical adducts remained the same (Table 5 and Figure 16). These differences were attributed to different photodegradation mechanisms in cellulose and BRW. Similarly, the impact of UV light on lignin-based carbon radicals was also studied by Grelier and co-workers and they proposed that hydroxyl (R-HO^\cdot) radicals formed first in a lignin system during exposure to UV in the presence of diradical molecular oxygen.^[91] Because these radicals are rather unstable, they are subsequently converted into carbon-centered radicals on the *meta* positions of a benzene ring. Successively, quinones are formed from these radicals, leading to yellowing of the outer layer of photodegraded

Table 5. DEPMPO radical adducts in wood or its components (after 1 h irradiation with UV light), as calculated from the simulated to experimental EPR spectra.^[89]

Entry	Substrate	Relative concentration [%]		
		HO [·]	HOO [·]	C-centered
1	wood	35.2	6.5	58.3
2	BRW	24.3	37.8	37.9
3	cellulose	48.5	15.7	35.8
4	wood + Cu ^{II} octanoate + ethanolamine	50.3	1.8	47.9
5	wood + Cu ^{II} sulfate	92.8	2.7	4.5

[a] BRW = brown rotted wood.

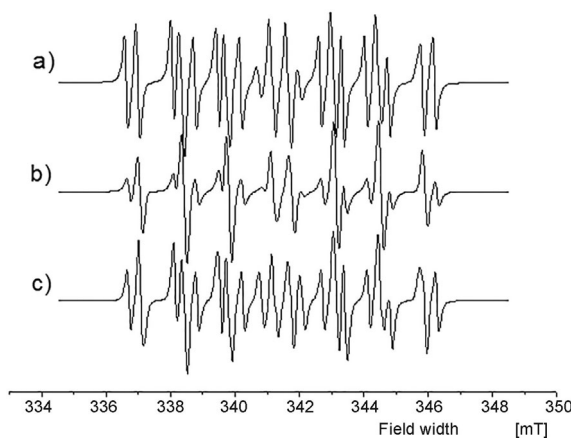


Figure 16. Simulated EPR spectra of DEPMPPO radical adducts (1 h irradiation, UV light) in a) wood, b) cellulose, and c) BRW. (Reprinted and adapted with permission from OCLC, Copyright, 2001–2016.)^[89]

wood.^[51] This research presented a valid argument regarding the impact of UV light, origin of lignin carbons radicals, and why a particular radical species dominates after light irradiation.

4.1. Spin-trapping ESR studies of unstable radicals from cellulose

So far, lignin radical intermediates after photodegradation have been discussed. Similar to lignin, it is believed that free radicals are also important intermediates during the process of photodegradation of cellulose.^[92] The effect of UV light on cellulose showed that the glycosidic linkages were cleaved, which resulted in the generation of free radicals at the C-1 and C-4 positions.^[93] A contrasting observation came from the analyses of cellulose radical intermediates. Because carbon-centered radicals in cellulose undergo secondary termination reactions, the hydroxyl radicals in cellulose are much more stable than those of carbon-centered radicals. This phenomenon helps to explain the observed higher amount of hydroxyl radical adducts in cellulose relative to carbon-centered radical adducts present in wood or lignin.

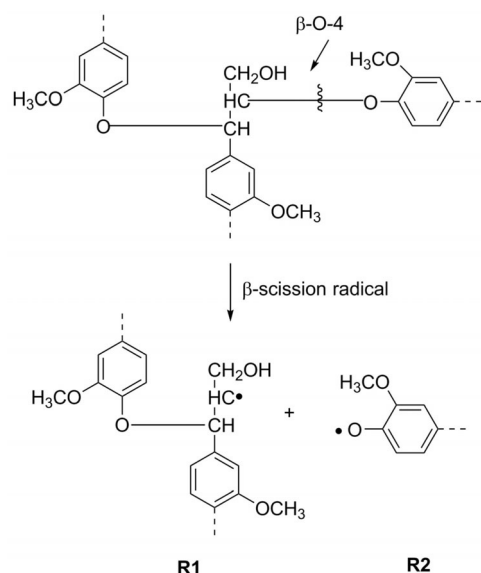
The role of copper as a protective shield against photodegradation for a wood surface is known in the literature.^[94,95] Elevated amounts of stable hydroxyl radicals in cellulose were attributed to the ability of copper present to protect hydroxyl radicals through the formation of stable adducts. From the data in Table 5 and Figure 15, it can be observed that, in the presence of copper(II) sulfate, primarily hydroxyl radical adducts were formed (93%); only 5% was designated to carbon-centered radical adducts and even less (ca. 3%) was designated to hydroperoxide radical adduct species. Similarly, the authors also observed that a less prominent reaction occurred in wood treated with copper(II) octanoate with ethanolamine (Table 5 and Figure 15). It was thus concluded that the development of carbon-centered radical adducts was prohibited. One hypothesis was that this could result from the probable trapping of copper(II) with free electrons during fragmentation

of hydroxyl radicals into carbon-centered radicals. The other hypothesis was that copper could provide resistance against UV degradation by blocking free phenol groups, which are prominent reactive sites for photochemical reactions. Copper(II) sulfate is more prone to adsorb on these groups than copper(II) octanoate with ethanolamine,^[96] and consequently, this justifies the observed difference between radical adducts.

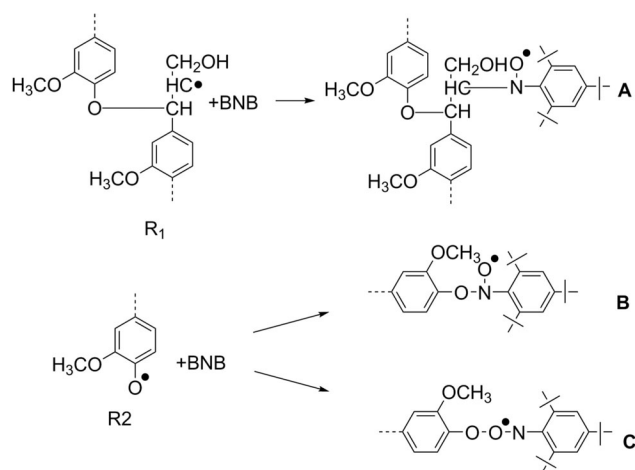
In summary, it was found that there are three forms of DEPMPPO-radical adducts that result from UV irradiation of wood or its components: hydroxyl (HO^\bullet), carbon-centered radical adducts, and hydroperoxide (HOO^\bullet) radical adducts. The various proportions of these radical adducts present in the UV-irradiated wood, cellulose, and lignin, indicated that different mechanisms were in operation. Although the treatment of wood with copper(II) was found to help to prevent the formation of carbon-centered and hydroperoxide radicals, significant amounts of hydroxyl radical adducts in copper(II)-treated wood were also observed.

So far, we have discussed hydroxyl and carbon radicals in wood, cellulose, and lignin. Similar to hydroxyl radicals, other oxygen-centered radicals also play an important role as radical intermediates in processes such as bleaching and assist in the generation of additional radical species.^[98,99] During bleaching, the scission of C–C bonds leads to the generation of radical species. For example, the efficient splitting of ether linkages (e.g., $\beta\text{-O-4}$) is of vital importance in pulping processes because of their impact on the quality of the pulp because they generate phenoxy and $-\text{CH}^\bullet$ radicals. A competent fabrication of high-quality pulp is essential because lignin-rich papers tend to yellow on the surface due to photo-oxidation. Therefore, these linkages in lignin leading to the generation of radical species are sought after for a detailed understanding of mechanisms involved in the processes. Although there is a plethora of reports on lignin model compounds and spin-trapping studies,^[82,100,101] there is a lack of discussion in the literature of the variety in spin trapping of radicals triggered directly from lignin. Among a few publications, to probe this aspect of lignin chemistry, Yoshioka et al. reported the homolytic fragmentation of alkyl phenyl ether bonds of hardwood and softwood lignin initiated by ultrasonic irradiation.^[102,103] The resulting radicals, such as secondary carbon ($-\text{CH}^\bullet$) and phenoxy radicals (Ph-O^\bullet ; Scheme 6, **R1** and **R2**) were short-lived, they were trapped by using the spin-trapping agent 2,4,6-tri-*tert*-butylnitrosobenzene (BNB), leading to the formation of stable adducts that are easily identified by ESR.

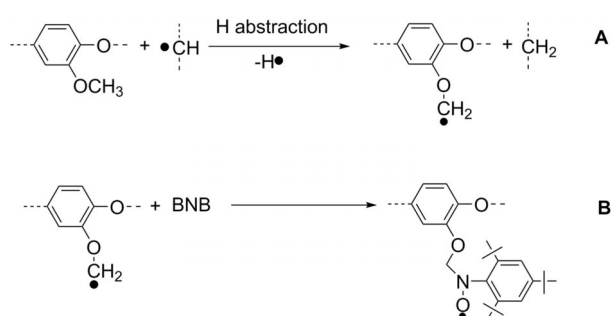
The spin-trapping reagent BNB is thought to function as follows: it forms a stable nitroxide adduct, $\text{R}(\text{N-O}^\bullet)$, with the $-\text{CH}^\bullet$ radical (Scheme 7A) and ESR parameters of $g=2.0065$, a nitrogen coupling constant (a^{N}) of 13 G, and a *meta*-hydrogen coupling constant (a^{H}) of 0.8 G.^[103] On the other hand, large radicals (e.g., *tert*-butyl radical) are trapped to generate an anilino adduct (R-N-O-C) with ESR parameters of $g=2.0045$, $a^{\text{N}}=10$ G, and $a^{\text{H}}=2$ G. The Ph-O^\bullet radical was not trapped as shown in Scheme 7C by BNB mainly because of the possible formation of extremely unstable peroxide species.^[103] Further data revealed that a primary carbon radical, OCH_2^\bullet , was trapped by BNB to form the respective stable adduct



Scheme 6. Probable structures generated from scission of β -O-4 linkages in lignin.^[97]



Scheme 7. Reported probable spin adducts generated after spin trapping with BNB.^[103]



Scheme 8. A) Formation of $\text{O}-\text{CH}_2\cdot$ radicals through H abstraction from $-\text{OMe}$ group. B) Trapping of $\text{O}-\text{CH}_2\cdot$ with spin-trapping BNB.^[103]

(Scheme 8). Thus, hydrogen atom abstraction from the *ortho*-methoxy groups in syringyl or guaiacyl moieties was initiated by the secondary carbon radical under ultrasonic irradiation

conditions. This was attributed to large steric hindrance effects operating between the syringyl with two methoxy groups and/or guaiacyl with a single methoxy group at the *ortho* position, and the BNB trap with two large *ortho-tert*-butyl groups.^[103] These rationalizations were in agreement with the thermally induced hemolytic cleavage of ether linkages and corresponding spin adducts with BNB.^[97]

5. Radical-Initiated Thermal Degradation and Cross-Linking in Lignin

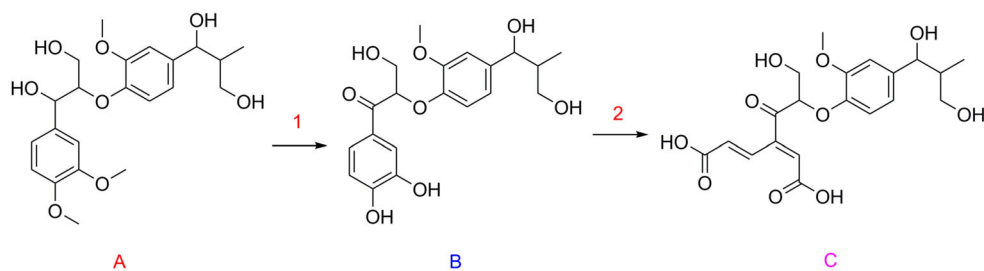
The formation of dissolved carbon-black matter originating from biochar residues (carbon black) has been gaining attention due to its detrimental impact on health and the environment.^[104,105] These dissolved carbon-black particles are composed of aliphatic and aromatic units substituted by aromatic C–O bonds, carboxylates, esters, and quinone moieties.^[106] The relationship between radically driven degradation of lignin and dissolved carbon-black matter has long been explored. Depending on the type of free radicals, their involvement in the process of degradation, gelation, and cross-linking are known to fluctuate. For example, oxidation triggered by hydroxyl radicals is capable of generating carbon-black matter, such as condensed organic compounds (see also Scheme 11).^[107] In particular, these hydroxyl radicals are believed to originate from photochemical reactions in aqueous systems and enzymatic microbial processes in soil.^[106,108–110] Because lignin plays a critical role in degradation processes, it is vital to investigate the various radical intermediates and their mechanisms in conjunction with each of these processes.

5.1. Role of hydroxyl and carboxyl radicals on degradation

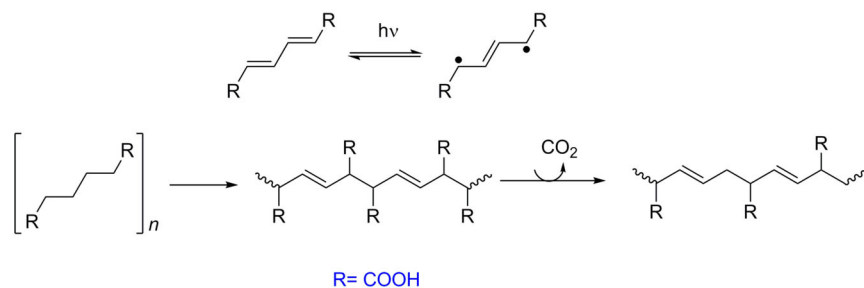
Hydroxyl radicals play a vital role because they are generated through ring opening, cyclization, hydrogen abstraction, and so forth in lignin. Hydroxyl radicals are known to react with dissolved carbon-black matter to produce low-molecular-weight acids, or to be mineralized entirely to CO_2 , along with oxidized organic compounds.^[112,113] Because lignin is accountable for a large portion of dissolved organic carbon-black matter and humic material, it is imperative to understand the process of lignin degradation through hydroxyl radicals and understand the formation of the corresponding degradation products.

Research by Waggoner et al. demonstrated that a lignin-rich extracted fraction of brown rotted wood produced hydroxyl radicals through Fenton chemistry in the absence of light.^[107] Both ^1H NMR spectroscopy and ultrahigh-resolution MS were employed to examine the bulk and molecular changes that resulted from exposure to hydroxyl radicals.

HRMS data showed additional changes from ring opening, carboxylation, and hydroxylation, which indicated the presence of new structures, and showed that several networks of structures emerged other than those shifted to higher oxygen and carbon ratios. One network had a higher hydrogen and carbon ratio (H/C) and lower oxygen to carbon ratio (O/C). This explained the presence of compounds that were detected to be



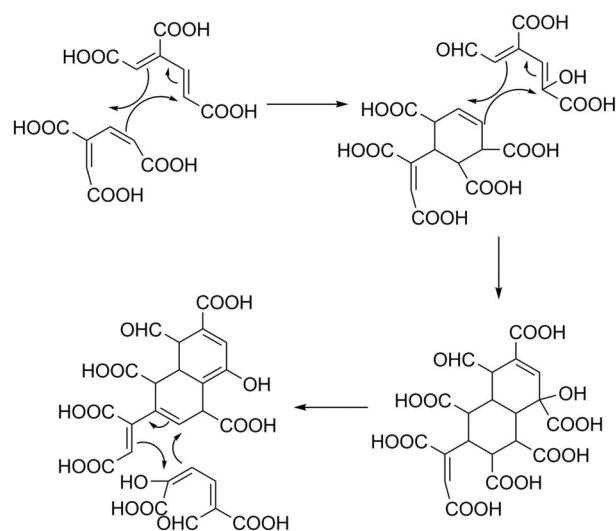
Scheme 9. Scheme representing 1) oxidation, depolymerization, and demethylation and 2) ring opening, leading to unsaturated aliphatic and hydroxylated carboxylic acid containing structure **C**.^[107,111]



Scheme 10. Possible radical polymerization during lignin degradation, leading to the formation of aliphatic polymeric compounds.^[107,114]

aliphatic in nature, with substantial oxygen functionality, that were likely to originate from carboxyl and hydroxyl groups (Scheme 9). This was in agreement with hydroxyl radical products with increased aliphatic resonances ($\delta = 2\text{--}3$ ppm). The unsaturated aliphatic carboxylic acids resulting from lignin modification (ring opening) shown in Scheme 9 are seen to play a key role in the formation of these compounds. Several reports have shown that unsaturated aliphatic acids are able to undergo polymerization through radical processes and generate long-chain aliphatic molecules with corresponding carboxyl groups (Scheme 10).^[114,115] These reports proposed that the loss of carboxyl groups from these chains resulted in compounds similar to those observed in the aliphatic region of ^1H NMR spectra.

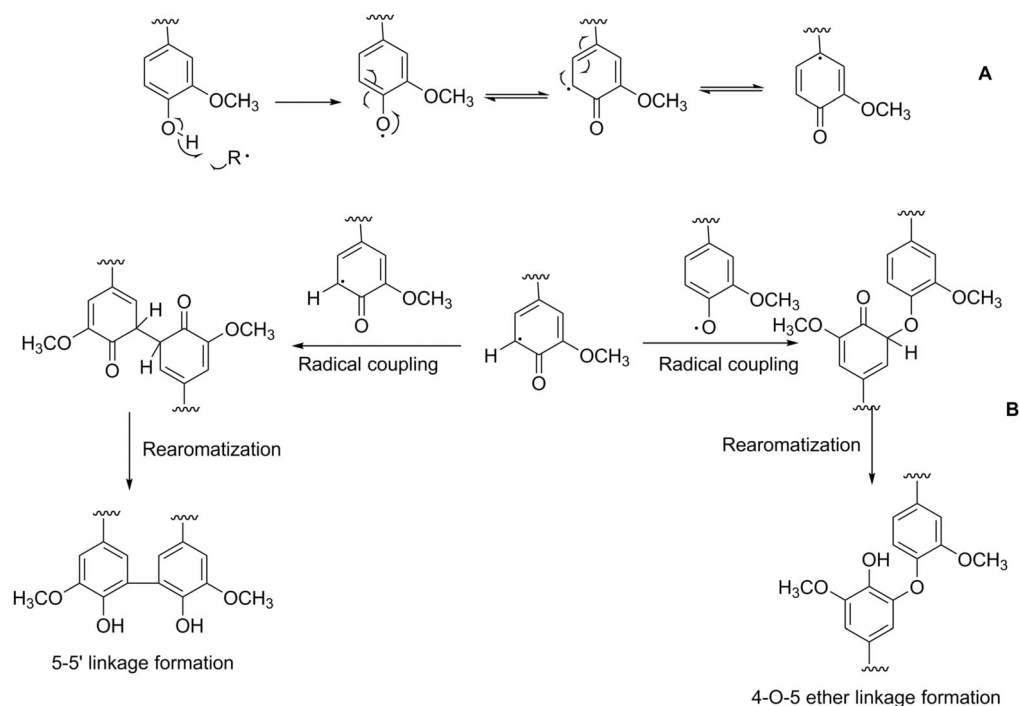
Additionally, a number of compounds with a molar hydrogen to carbon ratio less than 1.5, but still aliphatic in nature (ca. 200 formulae), showed formulae consistent with carboxyl-rich alicyclic molecules similar to those shown in Scheme 11, as described by Hertkorn et al.^[116] These alicyclic molecules were also believed to form through the radical polymerization processes described in Scheme 11, or through a process similar to that of cyclization, since it is known that unsaturated (hydroxylated) acids with extended conjugation readily undergo cyclization.^[117–119] Eventually, it was suggested that it might be possible to generate aliphatic/alicyclic acids^[120] through electrocyclic reactions (Scheme 11). All of these types of compounds matched reasonably in the observed range of H/C and O/C ratios ($\text{O/C} < 0.3$ and $\text{H/C} > 1.0$).



Scheme 11. Possible pathway for electrocyclization, leading to condensed aromatic and carboxyl alicyclic molecules.^[107]

5.2. Radical-initiated cross-linking in lignin

Lignin fragmentation at high temperatures ($> 200^\circ\text{C}$) is a widely used method and a plethora of literature is available on studies involved therein.^[121,122] Most reports available on the thermal degradation of lignin or model compounds indicate the involvement of radical intermediates in reaction mechanisms. One such report by Cui et al. described a possible pathway for processes occurring in lignin at thermoplastic processing temperatures ($< 200^\circ\text{C}$).^[123] This report assumed



Scheme 12. Possible thermally induced radical coupling reactions operating in kraft lignin triggered by radicals.^[123]

that radicals were stabilized and trapped by steric factors within the network of lignin and might be triggered at these temperatures.^[124] Thus, Cui et al. provided a probable explanation for the generation of phenoxy radicals through a hydrogen atom abstraction process when interacting with thermally activated radicals (R[•]). As such, it was hypothesized that these phenoxy radicals could undergo coupling reactions with the corresponding C5-centered mesomeric radical derivatives to form new 4-O-5 and 5-5' linkages, respectively (Scheme 12).

6. Summary and Outlook

The information assembled herein reveals that stable radicals are indisputably a critical part of lignin structure and play an important role in its chemistry. Their ubiquitous presence in lignin and their involvement in processes such as biodegradation, photo-oxidation, and fragmentation during chemical treatments, modifications, and pyrolysis have motivated researchers to investigate their origin, nature, and mechanisms of formation. This review is a step toward understanding the structures of stable radicals involved in lignin chemistry and paves the way to explore how various factors such as light, temperature, pH, and mechanical or chemical treatments of lignins play a pronounced effect on their radical content and structural details. For example, increases in radical content were observed with increasing fungal and chemical attack on native lignins. Hardwood lignins showed a higher spin content than softwood lignins. The photochemical production of quinones or the predominance of specific radical species is seen during lignin and wood pyrolysis. Furthermore, EPR spectroscopy (X-band EPR, LTMI-EPR, and high-field EPR), EPR spin-trap-

ping methods, and ³¹P NMR spectroscopy have confirmed the existence of persistent radicals in lignin and radical adducts that originate from key reactive radical intermediates. The method of spin trapping through EPR is an important technique for the observation and characterization of radicals involved in the photodegradation of wood and its components. Lignins subjected to alkali treatments, when examined by detailed EPR studies, revealed the presence of distinct quinhydrone systems, which showed that the extent of the quinone character depended on their spin contents.

In terms of gaps in our knowledge of this area, we consider a thorough understanding of the structure and nature of stable radical species in technical lignins to be of extreme significance. The use of X-band EPR HYSCORE spectroscopy, currently pursued in our work, reveals new information with pivotal technological ramifications.

Lignin is a highly abundant source of inexpensive and sustainable molecules that could be transformed into value-added biobased materials. Such conversions usually involve various pretreatments or chemical modifications, depending on the target application. Stable radicals in lignin are likely to play a critical role in imposing limitations that originate from their structure and reactivity. It is therefore imperative that our community becomes acutely aware of such species. This review is envisaged to serve as a platform to further delve into the structure and reactivity of such radical species.

Conflict of interest

The authors declare no conflict of interest.

Keywords: biomass · EPR spectroscopy · radicals · reactive intermediates · spin trapping

- [1] R. F. Gould in *Lignin Structure and Reactions, Vol. 59* (Ed.: J. Marton), ACS, Washington DC, **1966**, pp. i–iv.
- [2] K. M. Holtman, H.-M. Chang, H. Jameel, J. F. Kadla, *J. Agric. Food Chem.* **2003**, *51*, 3535–3540.
- [3] E. Adler, *Ind. Eng. Chem.* **1957**, *49*, 1377–1383.
- [4] S. E. Lebo, Jr., J. D. Gargulak, T. J. McNally, *Kirk-Othmer Encyclopedia of Chemical Technology*, 4th ed., Wiley, New York, **2001**.
- [5] C. Crestini, F. Melone, M. Sette, R. Saladino, *Biomacromolecules* **2011**, *12*, 3928–3935.
- [6] R. Vanholme, B. Demedts, K. Morreel, J. Ralph, W. Boerjan, *Plant Physiol.* **2010**, *153*, 895–905.
- [7] R. Whetten, R. Sederoff, *Plant Cell* **1995**, *7*, 1001–1013.
- [8] W. Boerjan, J. Ralph, M. Baucher, *Annu. Rev. Plant Biol.* **2003**, *54*, 519–546.
- [9] J. H. Grabber, *Crop Sci.* **2005**, *45*, 820–831.
- [10] F. S. Chakar, A. J. Ragauskas, *Ind. Crops Prod.* **2004**, *20*, 131–141.
- [11] Z. Strassberger, S. Tanase, G. Rothenberg, *RSC Adv.* **2014**, *4*, 25310–25318.
- [12] A. Bjorkman, *Nature* **1954**, *174*, 1057–1058.
- [13] V. K. Freudenberg, *Holzforchung* **1964**, *18*, 3–9.
- [14] V. K. Freudenberg, *Science* **1965**, *148*, 595–600.
- [15] V. K. Freudenberg, J. M. Harkin, *Phytochemistry* **1963**, *2*, 189–193.
- [16] V. K. Freudenberg, C. L. Chen, J. M. Harkin, H. Nimz, H. Renner, *Chem. Commun.* **1965**, *23*, 224–225.
- [17] V. K. Freudenberg, C. L. Chen, J. M. Harkin, H. Nimz, H. Renner, *Chem. Commun.* **1965**, *11*, 224–225.
- [18] V. K. Freudenberg, C.-L. Chen, G. Cardinale, *Chem. Ber.* **1962**, *95*, 2814–2828.
- [19] B. Chabbert, M. T. Tollier, B. Monties, Y. Barrière, O. Argillier, *J. Sci. Food Agric.* **1994**, *64*, 349–355.
- [20] J. L. McCarthy, *Ind. Eng. Chem.* **1957**, *49*, 1377.
- [21] R. W. Rex, *Nature* **1960**, *188*, 1185–1186.
- [22] D. S. Schonland, *Proc. Phys. Soc.* **1959**, *73*, 788.
- [23] W. Spackman, E. S. Barghoorn in *Coal Science, Vol. 55* (Ed.: P. H. Given), American Chemical Society, Washington, DC, **1966**, pp. 695–707.
- [24] V. K. Freudenberg, *Nature* **1959**, *183*, 1152–1155.
- [25] C. Steelink, T. Reid, G. Tollin, *J. Am. Chem. Soc.* **1963**, *85*, 4048–4049.
- [26] C. B. Purves, N. Levitan, N. S. Thompson, *Pulp Pap. Mag. Can.* **1955**, *56*, 117–130.
- [27] E. Adler, “Fourth International Congress of Biochemistry” **1959**, *11*, 137–145.
- [28] F. E. Brauns, *The Chemistry of Lignin*, Academic Press, New York, **1952**, pp. 15–20.
- [29] F. E. Brauns, D. A. Brauns, *The Chemistry of Lignin, Supplement Volume Covering the Literature of the Years 1949–1958*, Academic Press, New York, **1960**, pp. 179–189.
- [30] C. Steelink, *Geochim. Cosmochim. Acta* **1964**, *28*, 1615–1622.
- [31] C. Steelink, R. E. Hansen, *Tetrahedron Lett.* **1966**, *7*, 105–111.
- [32] C. Steelink in *Lignin Structure and Reactions, Vol. 59* (Ed.: J. Marton), ACS, Washington DC, **1966**, pp. 51–64.
- [33] J. Marton, *Tappi* **1964**, *47*, 713–719.
- [34] A. A. Dulov, B. I. Liogon’kii, A. V. Ragimov, A. A. Slinkin, A. A. Berlin, *Russ. Chem. Bull.* **1964**, *13*, 849–851.
- [35] N. C. Yang, Y. Gaoni, *J. Am. Chem. Soc.* **1964**, *86*, 5022–5023.
- [36] J. Law, M. Ebert, *Nature* **1965**, *205*, 1193–1196.
- [37] C. B. Colburn, R. Ettinger, F. A. Johnson, *Inorg. Chem.* **1963**, *2*, 1305–1306.
- [38] B. Košíková, K. Miklešová, V. Demianová, *Eur. Polym. J.* **1993**, *29*, 1495–1497.
- [39] *Lignins: Occurrence, Formation, Structural Reactions* (Eds.: K. V. Sarkanen, C. H. Ludwig), Wiley, New York, **1971**, pp. 328–350.
- [40] T. N. Kleinert, *Tappi* **1967**, *50*, 120.
- [41] J. D. Fitzpatrick, C. Steelink, *Tetrahedron Lett.* **1969**, *10*, 5041–5044.
- [42] C. Steelink, *J. Am. Chem. Soc.* **1965**, *87*, 2056–2057.
- [43] C. Bährle, T. U. Nick, M. Bennati, G. Jeschke, F. Vogel, *J. Phys. Chem. A* **2015**, *119*, 6475–6482.
- [44] Y. Matsunaga, *Can. J. Chem.* **1960**, *38*, 1172–1176.
- [45] J. Marton, E. Adler, *Acta Chem. Scand.* **1961**, *15*, 370.
- [46] H. Hatakeyama, J. Nakano, *Cell Chem. Technol.* **1970**, *4*, 281.
- [47] K. Kratzl, W. Schafer, P. Claus, J. Gratzl, P. Schilling, *Monatsh. Chem.* **1967**, *98*, 891.
- [48] T. Oniki, *Mokuzai Gakkaishi* **1997**, *43*, 493–498.
- [49] T. Oniki, U. Takahama, *Mokuzai Gakkaishi* **1997**, *43*, 499–503.
- [50] T. N. Kleinert, J. R. Morton, *Nature* **1962**, *196*, 334–336.
- [51] G. Leary, *Nature* **1968**, *217*, 672–673.
- [52] J. M. Pillinger, J. A. Cooper, C. J. Harding, *J. Chem. Ecol.* **1996**, *22*, 1001–1011.
- [53] J. Uebersfeld, A. Etienne, J. Combrisson, *Nature* **1954**, *174*, 614.
- [54] D. J. E. Ingram, J. G. Tapley, R. Jackson, R. L. Bond, A. R. Murnaghan, *Nature* **1954**, *174*, 797–798.
- [55] T. Ikoma, O. Ito, S. Tero-Kubota, K. Akiyama, *Energy Fuels* **1998**, *12*, 1363–1368.
- [56] T. Ikoma, O. Ito, S. Tero-Kubota, *Energy Fuels* **2002**, *16*, 40–47.
- [57] T. Ikoma, O. Ito, S. Tero-Kubota, K. Akiyama, *Energy Fuels* **1998**, *12*, 996–1000.
- [58] D. Cardona-Barrau, C. Matéo, D. Lachenal, C. Chirat, *Holzforchung* **2003**, *57*, 171.
- [59] P. Merdy, E. Guillon, M. Aplincourt, J. Dumonceau, H. Vezin, *J. Colloid Interface Sci.* **2002**, *245*, 24–31.
- [60] J. K. S. Wan, M. C. Depew, *Res. Chem. Intermed.* **1998**, *24*, 831–847.
- [61] M. Brai, A. Longo, A. Maccotta, M. Marrale, *J. Appl. Phys.* **2009**, *105*, 094913.
- [62] S. I. Kuzina, A. Y. Brezgunov, A. A. Dubinskii, A. I. Mikhailov, *High Energy Chem.* **2004**, *38*, 298–305.
- [63] J. Kibet, L. Khachatryan, B. Dellinger, *Environ. Sci. Technol.* **2012**, *46*, 12994–13001.
- [64] M. Carlier, J. P. Pauwels, L.-R. Sochet, *Oxid. Commun.* **1984**, *6*, 141–156.
- [65] L. Khachatryan, J. Adoukpe, B. Dellinger, *Energy Fuels* **2008**, *22*, 3810–3813.
- [66] R. K. Sharma, J. B. Wooten, V. L. Baliga, P. A. Martoglio-Smith, M. R. Haljaligol, *J. Agric. Food Chem.* **2002**, *50*, 771–783.
- [67] S. Zhou, Y. Xu, C. Wang, Z. Tian, *J. Anal. Appl. Pyrolysis* **2011**, *91*, 232–240.
- [68] W. A. Pryor, D. G. Prier, D. F. Church, *Environ. Health Perspect.* **1983**, *47*, 345–355.
- [69] T. M. Flicker, S. A. Green, *Environ. Health Perspect.* **2001**, *109*, 765–771.
- [70] A. Valavanidis, E. Haralambous, *Redox Rep.* **2001**, *6*, 161–171.
- [71] J. Adoukpe, L. Khachatryan, B. Dellinger, M. Ghosh, *Energy Fuels* **2009**, *23*, 1551–1554.
- [72] L. Khachatryan, J. Adoukpe, B. Dellinger, *J. Phys. Chem. A* **2008**, *112*, 481–487.
- [73] L. Khachatryan, R. Asatryan, C. McFerrin, J. Adoukpe, B. Dellinger, *J. Phys. Chem. A* **2010**, *114*, 10110–10116.
- [74] L. Khachatryan, J. Adoukpe, R. Asatryan, B. Dellinger, *J. Phys. Chem. A* **2010**, *114*, 2306–2312.
- [75] J. Adoukpe, L. Khachatryan, B. Dellinger, *Energy Fuels* **2008**, *22*, 2986–2990.
- [76] G. Leary, *J. Chem. Soc. Perkin Trans. 2* **1972**, 640–642.
- [77] C. Bährle, V. Custodis, G. Jeschke, J. A. van Bokhoven, F. Vogel, *ChemSusChem* **2014**, *7*, 2022–2029.
- [78] L. Zoia, R. Perazzini, C. Crestini, D. S. Argyropoulos, *Bioorg. Med. Chem.* **2011**, *19*, 3022–3028.
- [79] D. S. Argyropoulos, H. Li, A. R. Gaspar, K. Smith, L. A. Lucia, O. J. Rojas, *Bioorg. Med. Chem.* **2006**, *14*, 4017–4028.
- [80] L. Zoia, D. S. Argyropoulos, *J. Phys. Org. Chem.* **2009**, *22*, 1070–1077.
- [81] L. Zoia, D. S. Argyropoulos, *J. Phys. Org. Chem.* **2010**, *23*, 505–512.
- [82] L. R. C. Barclay, G. R. Cromwell, J. W. Hilborn, *Can. J. Chem.* **1994**, *72*, 35–41.
- [83] H. Karoui, F. Chaliier, J.-P. Finet, P. Tordo, *Org. Biomol. Chem.* **2011**, *9*, 2473–2480.
- [84] K. J. Liu, M. Miyake, T. Panz, H. Swartz, *Free Radical Biol. Med.* **1999**, *26*, 714–721.
- [85] A. Samuni, A. J. Carmichael, A. Russo, J. B. Mitchell, P. Riesz, *Proc. Natl. Acad. Sci. USA* **1986**, *83*, 7593–7597.
- [86] C. Frejaville, H. Karoui, B. Tuccio, F. L. Moigne, M. Culcasi, S. Pietri, R. Lauricella, P. Tordo, *J. Med. Chem.* **1995**, *38*, 258–265.

- [87] D. N.-S. Hon, S.-T. Chang, W. C. Feist, *Wood Sci. Technol.* **1982**, *16*, 193–201.
- [88] D. Fengel, G. Wegener, *Wood: Chemistry, Ultrastructure, Reactions*, de Gruyter, Berlin, **1989**, pp. 345–372.
- [89] M. Humar, M. Sentjurc, M. Petric, *Drvna Ind.* **2002**, *53*, 197–202.
- [90] F. S. Hosseinian, A. D. Muir, N. D. Westcott, E. S. Krol, *Org. Biomol. Chem.* **2007**, *5*, 644–654.
- [91] S. Grelier, A. Castellan, D. P. Kamdem, *Wood Fiber Sci.* **2000**, *32*, 196–202.
- [92] G. Buschle-Diller, S. H. Zeronian in *Photochemistry of Lignocellulosic Materials*, Vol. 531, American Chemical Society, Washington, DC, **1993**, pp. 177–189.
- [93] D. N. S. Hon, *J. Macromol. Sci. Phys.* **1976**, *10*, 1175–1185.
- [94] M. K. Yalınkılıç, R. İlhan, Y. Imamura, M. Takahashi, Z. Demirci, A. C. Yalınkılıç, H. Peker, *J. Wood Sci.* **1999**, *45*, 502–514.
- [95] R. Liu, J. N. R. Ruddick, L. Jin in *Int. Res. Group on Wood Pres. IRG/WP/94-30040*, 9, Nusa Dua, Bali, Indonesia, **1994**.
- [96] M. Petrič, R. J. Murphy, I. Morris, *Holzforschung* **2000**, *54*, 23–26.
- [97] T. Seino, A. Yoshioka, M. Takai, M. Tabata, *J. Appl. Polym. Sci.* **2004**, *93*, 2136–2141.
- [98] J. Gierer in *Lignin: Historical, Biological, and Materials Perspectives*, Vol. 742 (Eds.: W. G. Glasser, R. A. Northey, T. P. Schultz), American Chemical Society, Washington, DC, **1999**, pp. 422–446.
- [99] W. G. Glasser, R. A. Northey, T. P. Schultz in *Lignin: Historical, Biological, and Materials Perspectives*, Vol. 742 (Eds.: W. G. Glasser, R. A. Northey, T. P. Schultz), American Chemical Society, Washington, DC, **1999**, p. 580.
- [100] O. Lanzalunga, M. Bietti, *J. Photochem. Photobiol. B* **2000**, *56*, 85–108.
- [101] A. E. H. Machado, A. M. Furuyama, S. Z. Falone, R. Ruggiero, D. D. Perez, A. Castellan, *Chemosphere* **2000**, *40*, 115–124.
- [102] A. Yoshioka, T. Seino, M. Tabata, M. Takai, *Holzforschung* **2000**, *54*, 357–364.
- [103] T. Seino, A. Yoshioka, M. Fujiwara, K.-L. Chen, T. Erata, M. Tabata, M. Takai, *Wood Sci. Technol.* **2001**, *35*, 97–106.
- [104] E. Dons, L. I. Panis, M. Van Poppel, J. Theunis, G. Wets, *Atmos. Environ.* **2012**, *55*, 392–398.
- [105] N. A. Janssen, M. E. Gerlofs-Nijland, T. Lanki, R. O. Salonen, F. Cassee, G. Hoek, P. Fischer, B. Brunekreef, M. Krzyzanowski, *Environ. Health Perspect.* **2012**, *119*, 1691–1699.
- [106] H. Chen, H. A. N. Abdulla, R. L. Sanders, S. C. B. Myneni, K. Mopper, P. G. Hatcher, *Environ. Sci. Technol. Lett.* **2014**, *1*, 399–404.
- [107] D. C. Waggoner, H. Chen, A. S. Willoughby, P. G. Hatcher, *Org. Geochem.* **2015**, *82*, 69–76.
- [108] H. Fu, H. Liu, J. Mao, W. Chu, Q. Li, P. J. J. Alvarez, X. Qu, D. Zhu, *Environ. Sci. Technol.* **2016**, *50*, 1218–1226.
- [109] M. J. Pullin, S. Bertilsson, J. V. Goldstone, B. M. Voelker, *Limnol. Oceanogr.* **2004**, *49*, 2011–2022.
- [110] L. Sun, K. Mopper, *Front. Mar. Sci.* **2016**, *2*, 117.
- [111] A. C. Stenson, A. G. Marshall, W. T. Cooper, *Anal. Chem.* **2003**, *75*, 1275–1284.
- [112] T. Heitmann, T. Goldhammer, J. Beer, C. Blodau, *Global Change Biol.* **2007**, *13*, 1771–1785.
- [113] S. E. Page, G. W. Kling, M. Sander, K. H. Harrold, J. R. Logan, K. McNeill, R. M. Cory, *Environ. Sci. Technol.* **2013**, *47*, 12860–12867.
- [114] A. Matsumoto, K. Yokoi, S. Aoki, K. Tashiro, T. Kamae, M. Kobayashi, *Macromolecules* **1998**, *31*, 2129–2136.
- [115] A. Matsumoto, T. Matsumura, S. Aoki, *Macromolecules* **1996**, *29*, 423–432.
- [116] N. Hertkorn, R. Benner, M. Frommberger, P. Schmitt-Kopplin, M. Witt, K. Kaiser, A. Kettrup, J. I. Hedges, *Geochim. Cosmochim. Acta* **2006**, *70*, 2990–3010.
- [117] O. Diels, K. Alder, *Justus Liebigs Ann. Chem.* **1928**, *460*, 98–122.
- [118] J. G. Martin, R. K. Hill, *Chem. Rev.* **1961**, *61*, 537–562.
- [119] P. N. Devine, T. Oh, *J. Org. Chem.* **1992**, *57*, 396–399.
- [120] J. M. Harris, C. C. Wamser, *Fundamentals of Organic Reaction Mechanisms*, Wiley, New York, **1976**, pp. 192–198.
- [121] M. J. Antal in *Advances in Solar Energy: An Annual Review of Research and Development*, Vol. 2 (Eds.: K. W. Böer, J. A. Duffie), Springer, Boston, **1985**, pp. 175–255.
- [122] M. Brebu, C. Vasile, *Cellul. Chem. Technol.* **2010**, *44*, 353–363.
- [123] C. Cui, H. Sadeghifar, S. Sen, D. S. Argyropoulos, *BioResources* **2013**, *8*, 864–886.
- [124] Y. N. Sazanov, A. V. Gribanov, *Russ. J. Appl. Chem.* **2010**, *83*, 175–194.

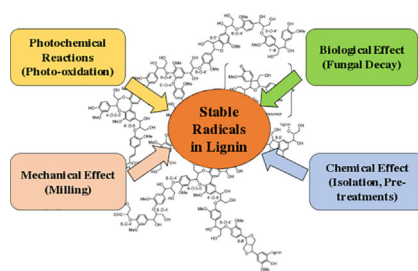
Manuscript received: May 18, 2017

Accepted manuscript online: June 12, 2017

Version of record online: ■■■■■, 0000

REVIEWS

Secrets hidden in the wood: Lignin and the quest for the origin of stable organic radicals in it have seen numerous developments. The extreme complexity of lignin and its highly aromatic, cross-linked, branched, and rigid structure has made such efforts rather cumbersome. Herein, the factors contributing to the formation of stable radicals in lignin are discussed.



S. V. Patil, D. S. Argyropoulos*



Stable Organic Radicals in Lignin: A Review